*Journal of Systematic Palaeontology* **4** (2): 157–184
doi:10.1017/S1477201905001719 Printed in the United Kingdom
Issued 1 June 2006


# Description and systematic relationships of †*Tomognathus*, an enigmatic fish from the English Chalk

**Peter L. Forey**
Department of Palaeontology, The Natural History Museum, Cromwell Road, London SW7 5BD, UK

**Colin Patterson**
Deceased*

**SYNOPSIS** The Upper Cretaceous fish †*Tomognathus mordax* Dixon, 1850, is redescribed, based on newly acid-prepared material that reveals many new structures and reinterpretations of some parts of anatomy previously described. The cranium shows the absence of a supraoccipital, a double jaw joint involving a symplectic and quadrate, a lower jaw incorporating a coronoid, prearticular and a surangular, concave shape of the posterior margin of the maxilla, a single supramaxiila, a 'V'-shaped median rostral with lateral horns and an interopercle that lies in series with the subopercle. These features suggest affinities with the Halecomorphi. Within Halecomorphi, character conflict means that †*Tomognathus* may only be placed as Superfamily Amioidea *incertae sedis*. It is highly apomorphic in showing parietals, frontals, premaxillae and vomers all fused into median elements, a parasphenoid with scythe-like processes developed along the ascending wings and an infraorbital series reduced to tube-like elements. †*Tomognathus* is one of only three halecomorphs recorded from the English Chalk.

**KEY WORDS** anatomy, Halecomorphi, Upper Cretaceous, Amioidea

## Contents



* Note on authorship: During the early 1970s Colin Patterson (1933–1998) acid-prepared several specimens of †*Tomognathus* to reveal several well preserved braincases and disarticulated skull elements. He also produced several drawings (Figs 3C, 4, 5, 7, 8 & 9). However, no notes accompanied this work. The drawings are to his usual high standard and it seems an act of omission to leave them unrecorded in a drawer. Therefore, I have recovered them, added to them and provided a description and discussion of the phylogenetic position of this hitherto enigmatic fish. P.L.F.

## Introduction

In 1850 Frederick Dixon described a very unusual fish from the English Chalk. He had at his disposal one head about 5 cms long and one small jaw. Both showed very prominent teeth and he named the genus †*Tomognathus* (Greek = 'incisor jaw') giving the specific name *mordax* (Latin = 'biting') to the head specimen (Fig. 1A). He thought that the teeth in the small jaw specimen were smoother than those in the type specimen and he coined the name †*T. leiodus* (Greek = 'smooth') for the small jaw (Fig. 1B). Dixon made no observation as to what kind of fish he was dealing with. Woodward (1901) briefly redescribed †*Tomognathus* and, with an increased sample of 30 specimens, some of which intergraded in tooth structure between those shown by the original two, he affirmed his earlier suspicion (Woodward 1888: 313) that there was only one species – †*T. mordax*. Woodward (1901: 116) placed †*Tomognathus* as a questionable chirocentrid, which in his day meant closely related to ichthyodectiforms (at the turn of the 20th century ichthyodectiforms were included with the modern clupeomorph *Chirocentrus*, or wolf-herring). Woodward (1908) later changed his mind and, in providing a longer description, he erected a new monospecific family †Tomognathidae, which he allied with stomiiform fishes and maintained this view in a further publication (Woodward 1936). Stomiiforms are a group of mid- and deep water marine teleosts represented today by the snaggletooths and dragonfishes. The comparisons are obvious and understandable given the large fang-like teeth in †*Tomognathus*. Therefore, since †*Tomognathus* had been discovered the suggested affinities of this fish had shifted from unknown, to a teleost stem representative, to deep within euteleosts.

Our current ideas on the phylogeny of teleosts predicts that stomiiforms should be present in the Albian but the earliest undoubted member known by skeletal material is †*Astronesthes praevius* from the Lutetian of Georgia (Patterson 1993). Therefore the suggestion that †*Tomognathus* may be a stomiiform is of some interest. However, the synapomorphies of stomiiforms (Fink & Weitzman 1982; Harold & Weitzman 1996) are mostly soft tissue characters, which are usually unavailable in fossils, as well as detailed structure of the cartilage ends of the upper pharyngeal elements which are, at best, difficult to restore in fossils. One character – attachment of some branchiostegal rays to the ventral hypohyal – is potentially observable but this region of the skeleton has not yet been seen in †*Tomognathus*. Furthermore, if †*Tomognathus* is related to stomiiforms it may be expected to show at least some of the synapomorphies that specify the intervening nodes along the base-line of teleostean phylogeny. Some of the more obvious of these are indicated in Fig. 2.

The availability of acid-prepared material now allows a much more complete description of the cranial anatomy of †*Tomognathus* (the postcranial skeleton remains largely unknown). This permits a more accurate assessment of the phylogenetic position of †*Tomognathus*. To anticipate the conclusion of this paper, it is now clear that †*Tomognathus* has nothing to do with teleost fishes but is related to amioids and must, therefore, be placed as another halecomorph.

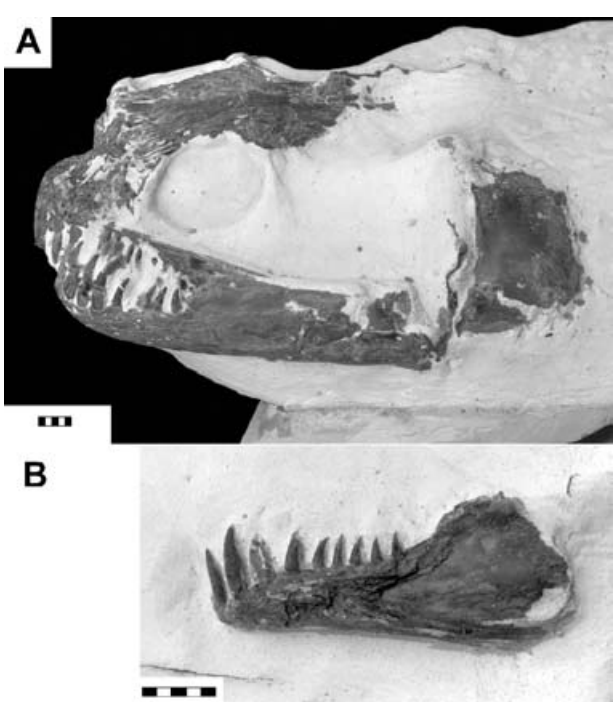


**Figure 1** Holotype specimens. **A**, †*Tomognathus mordax* Dixon, 1850, holotype, BM 007225: **B**, †*Tomognathus leiodus* Dixon, 1850, holotype, BMNH 25925. Scale bars = 5 mm.

### Methods

Specimens were prepared using the needle and acid transfer method (Toombs & Rixon 1959). In some of the illustrations interpretative line drawings are given alongside photographs. In all instances the drawings were made directly from the specimens rather than from the photograph. This was found to be more accurate but it means that for some a slightly different angle of view may be apparent. The camera lucida drawings were made using a Wild M7 microscope and drawing tube.

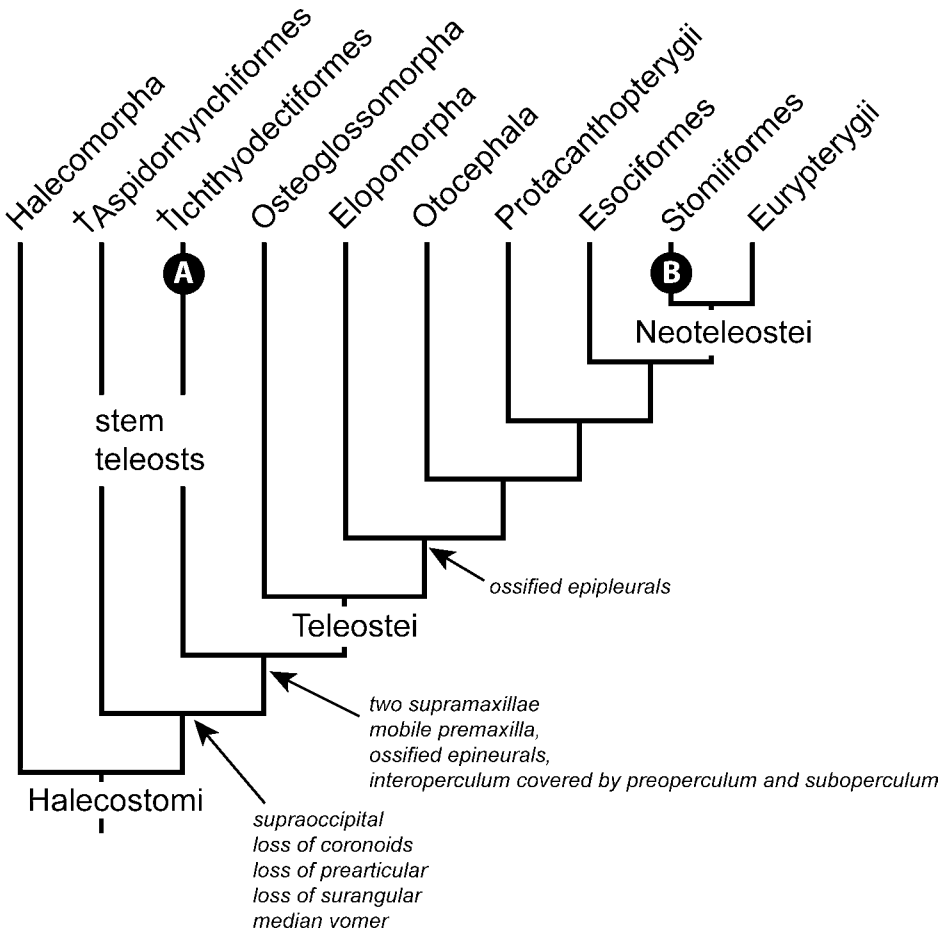


**Figure 2** Previous ideas on the relationships of †*Tomognathus*. Outline phylogeny of halecostome actinopterygians showing two suggested phylogenetic placements of †*Tomognathus* (circles): **A**, Woodward (1901) considered †*Tomognathus* to be a chirocentrid (equivalent at that time to ichthyodectiforms); **B**, Woodward (1908) placed †*Tomognathus* with stomiiform neoteleosts. Given either of these ideas we would expect †*Tomognathus* to show some of the many synapomorphies supporting the nodes subtending †Aspidorhynchifomes to Eurypterygii. Those relating to parts of the skeleton present in the known remains of †*Tomognathus* are shown at their relevant hierarchical level. †*Tomognathus* shows only one of these (median vomer), raising the possibility that it may be a basal stem teleost. However, it is argued in this paper that there are several characters suggesting that it is nested within halecomorphs. Many of the characters supporting the nodes in this tree (including crown group Teleostei) are variations in features of the caudal endoskeleton, branchial and hyoid arches or soft anatomy.

## Material

In the following text, specimens from four institutions are used. The institutional abbreviations preceding specimen numbers are as follows: **BMNH**, The Natural History Museum, London; **BM**, Booth Museum, Brighton; **SM**, Sedgwick Museum, Cambridge University; **ZMC**, Zoology Museum, Cambridge University.

## Abbreviations used in text figures

**Ang**, angular; **Ao**, antorbital; **Art**, articular; **art.Mx**, articulatory surface for maxilla; **art.Pal**, articulatory surface for palatine; **a.sc.c**, recess for anterior semicircular canal; **asc.Par**, ascending process of parasphenoid; **Asph**, autosphenotic; **Boc**, basioccipital; **B.r**, branchiostegal ray(s); **Brp**, branchopercle; **Bsph**, basisphenoid; **can.so.s.c**, canal for supraorbital sensory canal; **Ch.a**, anterior ceratohyal; **ch.sac**, saccular chamber; **ch.utr**, utricular chamber; **c.j.v**, canal for jugular vein; **Cle**, cleithrum; **Co**, coronoid; **cr.Fr**, frontal crest; **cr.Pa**, parietal crest; **Den**, dentary; **Dpal**, dermopalatine; **Dsph**, dermosphenotic; **Ecpt**, ectopterygoid; **Enpt**, entopterygoid; **Epo**, epioccipital; **Eth**, ethmoid; **Exo**, exoccipital; **fac.Hm**, facet for hyomandibular; **f.add**, adductor fossa in lower jaw; **f.i.c.a**, foramen for internal carotid artery; **f.m**, foramen magnum; **f.mx.V**, foramen for maxillary branch of trigeminal nerve; **f.occ.a**, foramen for occipital artery; **f.o.n.a**, foramen for orbitonasal artery; **fos.ptt**, posttemporal fossa; **f.ot.VII**, foramen for otic ramus of the facial nerve; **Fr**, frontal; **f.s.oph**, foramen for superficial ophthalmic (anterior dorsal lateral line nerve); **f.I**, foramen for olfactory tract; **f.II**, foramen for optic tract; **f.III**, foramen for oculomotor nerve; **f.IV**, foramen for trochlea nerve; **f.V**, foramen for trigeminal nerve; **f.VI**, foramen for abducens nerve; **f.VII.hm**, foramen for hyomandibular branch of VII; **f.VII.h + j.v**, foramen for hyomandibular branch of facial nerve and jugular vein; **f.VII.pal**, foramen for palatine branch of facial nerve; **f.IX**, foramen for glossopharyngeal nerve; **f.X**, foramen for vagus nerve; **gle**, articulatory glenoid; **gr.j.v**, groove for jugular vein; **Hm**, hyomandibular; **Ic**,

intercalar; **Inf**, infraorbital (numbered); **Iop**, interopercle; **Mpt**, metapterygoid; **m.s.c**, mandibular sensory canal; **Mx**, maxilla; **my.p**, posterior myodome; **Na**, nasal; **nos.a**, notch for anterior nostril; **n.pr.Pmx**, nasal processes of premaxilla; **occ.con**, occipital condyle; **Op**, opercle; **o.ot.s.c**, opening for otic sensory canal; **Ors**, orbitosphenoid; **o.so.s.c**, opening for supraorbital sensory canal; **Pa**, parietal; **Par**, parasphenoid; **Pmx**, premaxilla; **Pop**, preopercle; **Prart**, prearticular; **pr.a.Par**, anterior process on ascending process of parasphenoid; **Pro**, prootic; **Pro.br**, prootic bridge; **pr.Op**, opercular process; **pr.p.Pmx**, posterior process of the premaxilla; **pr.Sy**, symplectic process; **p.sc.c**, recess for posterior semicircular canal; **Pto**, pterotic (dermopterotic); **Pts**, pterosphenoid; **Qu**, quadrate; **Retr**, retroarticular; **Ros**, rostral; **Sang**, surangular; **Sca.cor**, scapulocoracoid; **Smx**, supramaxilla; **Sop**, subopercle; **so.s.c**, supraorbital sensory canal; **Sy**, symplectic; **t.Pmx**, premaxillary tooth (teeth); **tp.Enpt**, tooth patch on entopterygoid; **t.Prart**, prearticular teeth; **Vo**, vomer.

## Systematic Description

Subclass **ACTINOPTERYGII** Cope, 1887

Series **NEOPTERYGII** Regan, 1923 (*sensu* Rosen *et al.*, 1981)

Division **HALECOSTOMI** Regan, 1923 (*sensu* Patterson, 1973)

Subdivision **HALECOMORPHI** Cope, 1872 (*sensu* Patterson, 1973)

Order **AMIIFORMES** Hay, 1929 (*sensu* Grande & Bemis, 1998)

Superfamily **AMIOIDEA** Bonaparte, 1838 (*sensu* Grande & Bemis, 1998)

Family **Incertae Sedis**

Genus †***TOMOGNATHUS*** Dixon, 1850

Diagnosis (emended). Amioidea with median parietals bearing a crest, median frontals; fused premaxillae with a posterior ventral process that sutures with an unpaired vomer, ascending processes of the premaxilla failing to enclose foramen for the olfactory tract completely, parasphenoid edentulous with scythe-like processes on the ascending processes, no basipterygoid process, opisthotic absent, intercalar represented by membrane bone only, occipital condyle formed by basioccipital and exoccipitals; one coronoid in lower jaw bearing a single row of teeth, prearticular with single row of teeth; palate with single dermopalatine; double jaw joint in which the quadrate and symplectic contributions are very close to one another forming a single functional unit; gular plate fan-shaped, with fine ridges radiating from an anteriorly placed ridge and ending in a pectinated posterior margin; no supraorbitals or suborbitals, infraorbitals tube-like, dermosphenotic free from skull roof and lying well in advance of the autosphenotic; dorsal fin long, beginning immediately behind the head and extending most of the length of the body.

Type and only species. †*Tomognathus mordax* Dixon, 1850.

†***Tomognathus mordax*** Dixon, 1850 (Figs 1, 3–20)

1850 †*Tomognathus mordax* Dixon: 376, pl. 35, fig. 1.
1850 †*Tomognathus leiodus* Dixon: 377, pl. 30, fig. 31.
1888 †*Tomognathus mordax* Dixon; Woodward: 31.
1901 †*Tomognathus mordax* Dixon; Woodward: 117.
1908 †*Tomognathus mordax* Dixon; Woodward: 139, pl. 29, figs 3–13.
1936 †*Tomognathus mordax* Dixon; Woodward: 304, pl. 6.

Diagnosis. As for genus, only species.

Holotype. BM 007225 head (Fig. 1A), Lower Chalk, Clayton, West Sussex.

Remarks. Woodward (1908: 139) maintained that the type specimen had been lost. This is not the case.

Material. All of the material referred to this taxon comes from the Cenomanian and Turonian of south east England. In some cases locality and stratigraphic information is minimal. Historically, several different specimens were originally given the same register number and recorded as such in Woodward's (1901) catalogue. We choose this opportunity to give each a unique number and this is recorded below.

Lower Chalk, Kent: BMNH 36172, 37325, 39050 (figured Woodward 1908: pl. 29, fig. 6), 41684, 47242, 47917, 49058, 49092, P.1701 (figured Woodward 1908: pl. 29, fig. 12), P.1702, P.5675, P.5676, P.7646 (figured Woodward 1908: pl. 29, fig. 3), P.9043 (figured Woodward 1908: pl. 29, fig. 9), P.10632 (figured Woodward 1908: pl. 29, fig. 13), P.11799, P.16950, P.16951, P.65654 (formerly part of P.1702), P.65655 (formerly part of P.1702), P.65656 (formerly part of P.7676), P.65659 (formerly part of P.1702), P.65660 (formerly part of P.6576), SM B.9161.

Surrey: BMNH 49767, 49768.

Sussex: BM 007227, 007226; BMNH 25925 (Holotype of *T. leiodus* Dixon, 1850, figured Dixon 1850: pl. 30, fig. 31), 49761, 49762 (figured Woodward 1908: pl. 29, fig. 4), 49763, 49764, 49765, 49766, 49769, P.3849, P.20122 (figured Woodward 1936: pl. 6), P.65661 (formerly part of 25925), P.65662 (formerly part of P.3849), P.65663 (formerly part of P.3849), P.65664 (formerly part of P.3849), SM B.9164.

South east England: BMNH 25801, 25813, 39051, 49080, P.4791, P.4844 (figured Woodward 1908: pl. 29, figs 7, 8, 10), P.6460, P.6460a, P.9237 (figured Woodward 1908: pl. 29, fig. 5), P.65657, P.65658, BM 016968, SM B.9162, B.9163, B.75729, B75730, ZMC GN 543

Remarks on other localities. It is possible that †*Tomognathus* occurs in the Turonian Chalk of the Czech Republic (Ekrt 2001). Frič (1879) described a specimen from the Turonian of Bílá hora, near Prague, under the name *Istieus spottii*. Frič & Bayer (1902) and Fritsch & Bayer (1905) recognised that it did not belong to the genus *Istieus* (an albulid fish) and hence erected the generic name *Denticopsis* to contain *D. spottii*. The single holotype specimen exists in the Natural History Museum, Prague, where it is represented by a disarticulated head and parts of the dorsal and pectoral fins. The specimen is largely a natural mould and therefore details are poor. However, the jaw looks very similar to that of †*Tomognathus mordax* and it may well be conspecific. We

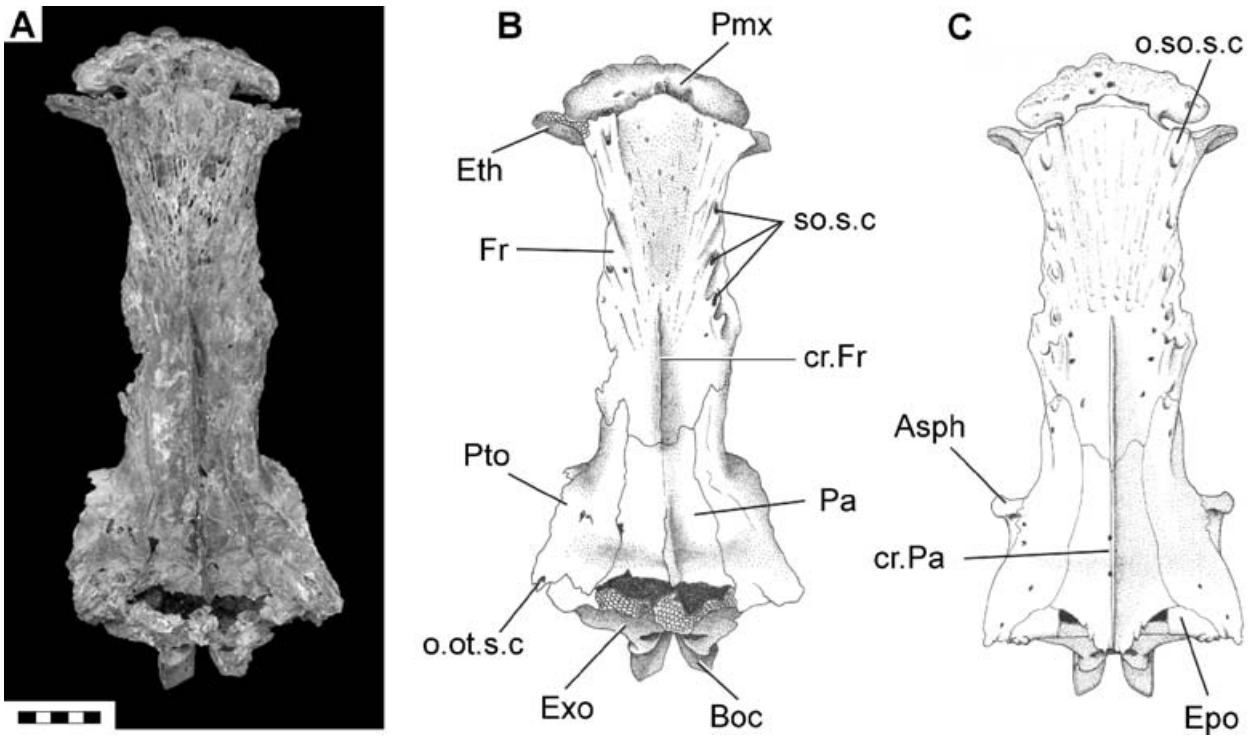


**Figure 3** †*Tomognathus mordax* Dixon, 1850, skull roof. **A**, dorsal view of braincase of BMNH P.11799; **B**, interpretive drawing of BMNH P.11799; **C**, restoration of skull roof based on BMNH P.11799 with additional information from BMNH 49761 and 49765. Scale bar = 5 mm.

have not seen the specimen and therefore are reluctant to formally place it in synonymy.

## Description

### Braincase

The braincase is blunt-snouted, deep throughout its length with a dorsally domed otic region that is keeled ventrally. In dorsal view (Fig. 3) the roof is parallel-sided above the orbit; it flares anteriorly towards the ethmoid region and posteriorly at the rear limit of the skull. Unlike most members of the Halecomorphi the skull roofing bones are unornamented, except for minor rugosities and the skull roof is strongly vaulted with a median crest. In most halecomorphs the skull roof is flat and the presence of ornament in most suggests that it was covered with a thin layer of skin only. We suspect that, in life, the skull roof of †*Tomognathus* would have been deeply buried within skin and muscle.

The frontals (see Figs 3, 7, 9 & 13: **Fr**) are fused in the mid line and together make up the largest elements in the skull roof. Ornamentation is confined to a series of irregular grooves that fan out anteriorly. The lateral margin is very irregular but shows a minor flare at mid orbital level. We are uncertain if the fused frontal condition is ontogenetic or phylogenetic; but all specimens showing the skull roof show fused frontals and this condition must be regarded as typical for this species. This is unlike the condition for *Amia calva* where Grande & Bemis (1998) found one specimen in 119 examined that showed this condition. Fused frontals are relatively rare in actinopterygians but the condition is known in eels: in fact Regan (1912) separated Recent eels into two major groups based on the presence of paired (e.g. anguilloids) or fused frontals (e.g. congroids and synaphobranchoids). The fused frontals are parallel-sided; that is, they are not posteriorly flared as is the usual teleostean condition (Arratia & Schultze 1987). Close to the lateral margins of the fused frontals there is a series of six pores (Fig. 3: **so.s.c**) opening from the supraorbital sensory canal, the latter opens at the extreme anterior end of the frontal through a large pore leading from a prominent tube (Figs 3 & 4: **o.so.s.c**), somewhat similar to that seen in †*Calamopleurus cylindricus* (Grande & Bemis 1998: fig. 297). In some specimens the posterior opening is double. In the posterior half of the fused frontals a median crest (see Figs 3, 4B, 6 & 8B: **cr.Fr**) continues that on the parietals. This reaches to mid orbital level before it gives way to a shallow median depression.

The parietals are also fused into a median element (see Figs 3 & 6: **Pa**) and developed as a prominent median crest (see Figs 3C, 6, 8A & 15: **cr.Pa**), particularly obvious in lateral view and, in life, no doubt provided a large area for the insertion of epaxial musculature. The parietal is long and narrow – the median width being equal to half of the length. Sutures with the frontal anteriorly, the pterotic laterally and the epioccipital posteriorly are simple. The posterior margin of the parietal is of complex shape. A small lacuna is left between the parietal, epioccipital and the dorsal cartilage lined surface of the exoccipital (Fig. 3B). It is probable that this space was occupied with cartilage in life. A median parietal is rare but is a character of †Sinamiidae (†*Ikechaoamia* and †*Sinamia*, see Grande & Bemis 1998: 583), where it is represented by an flat, equidimensional bone without a median crest. A median parietal is also present in *Amia* as an anomaly, but this cannot be regarded as characteristic of this

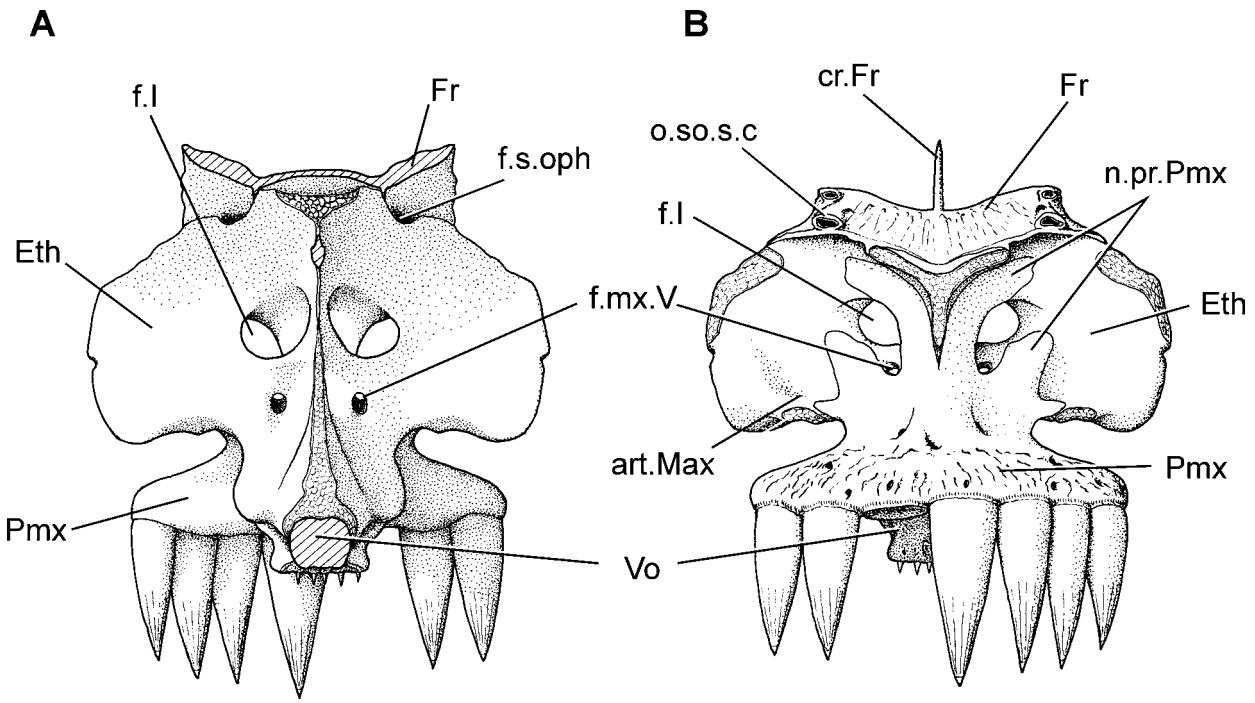


**Figure 4** †*Tomognathus mordax* Dixon, 1850. Ethmoid region. **A**, reconstruction in posterior view; **B**, in anterior view. Based on BMNH 49761, 49765 and P.11799. Approximately × 4 natural size.

species (*contra* Arratia 1999: table 1, character 3, state 1). Grande & Bemis (1998) discuss the occurrence of a median parietal in *Amia* noting that in their sample of 119 specimens the condition occurred in one individual and, therefore, was regarded as a teratological phenomenon. A median parietal is found in most ichthyodectiforms, a group with which †*Tomognathus* was once associated. In ichthyodectiforms there is an associated supraoccipital that divides most of the median parietal into left and right limbs. The pterotic (see Figs 3, 6 & 15: **Pto**) is paired; it flanks the parietal and extends forward to suture with the frontal above the orbit. It forms the roof of a shallow posttemporal fossa (see Fig. 8A: **fos.ptt**). Some specimens (e.g. BMNH P.4844) show small pores leading from the otic sensory canal.

A note on previous identifications of the skull roofing bones is in order. Woodward (1936) identified the fused parietals as the supraoccipital and the pterotics as the parietals. (Interestingly, Grande & Bemis (1998: 39) record that Bridge (1877) made the same identification for an anomalous specimen of *Amia calva*.) Woodward's (mis)identification is perfectly understandable in the context in which he was describing †*Tomognathus*. In thinking that †*Tomognathus* was a teleost he naturally likened a posteriorly placed, median roofing bone to a supraoccipital (a teleost synapomorphy), a bone commonly developed as a crest. That this is not the case in †*Tomognathus* is evidenced by four criteria: (1) the median element in †*Tomognathus* is entirely dermal (in some teleosts the endochondral supraoccipital does have a dermal component, usually thought to have come about by phylogenetic/ontogenetic fusion of extrascapulars; the supraoccipital would therefore be a canal-bearing bone unlike the canal-free bone in †*Tomognathus*); (2) it fails to contribute to the posterior face of the braincase; (3) it has no association with the semicircular canals (a supraoccipital is endochondral, contributes to the posterior face of the braincase in at least lower teleosts and is usually pierced by the posterior semicircular canals); (4) the lateral elements carry the otic sensory canal and suture with the autosphenotics (attributes of a pterotic). There is no evidence of an ossified endochondral supraotic bone as occurs in some halecomorphs (Maisey 1999).

The anterior part of the braincase is formed by the ethmoid and the premaxilla, together with nasals, rostral and antorbital (these latter three bones are described later). In all specimens the ethmoid (see Figs 3–6 & 15: **Eth**) is a complex single element that covers the territory occupied by the paired lateral ethmoids and pre-ethmoids of *Amia* (Grande & Bemis 1998: fig. 22). Although the complex shape of this bone suggests that it ossified from more than one centre there is no indication of separate elements in any specimen available to us. The ethmoid forms the anterior wall of the orbit and, at the same time, the posterior wall of the nasal capsules. It is developed laterally as two broad wings that have small areas of unfinished bone both dorsally and ventrally. Ventrally there are two small areas, both at the tips of small projections, placed one behind the other and best seen in ventral view (Fig. 5). These provided articulation points for the inturned head of the maxilla (Figs 5 & 6: **art.Mx**) and the autopalatine (Figs 5 & 6 **art.Pal**) (see below). The significance of the unfinished area on the dorsal surface of the ethmoid is unclear. The dorsal portion of the ethmoid continues forward as a thin lamina that is 'T'-shaped in anterior view (see Figs 4B & 13) and terminates in unfinished bone, again suggesting that in life this would have been capped with cartilage. The posterior surface of the ethmoid is developed as a thin, median interobital septum that sutures with the orbitosphenoid posteriorly. This posterior lamina is often perforated by fenestrae, but these are variously developed from specimen to specimen, suggesting that they are without

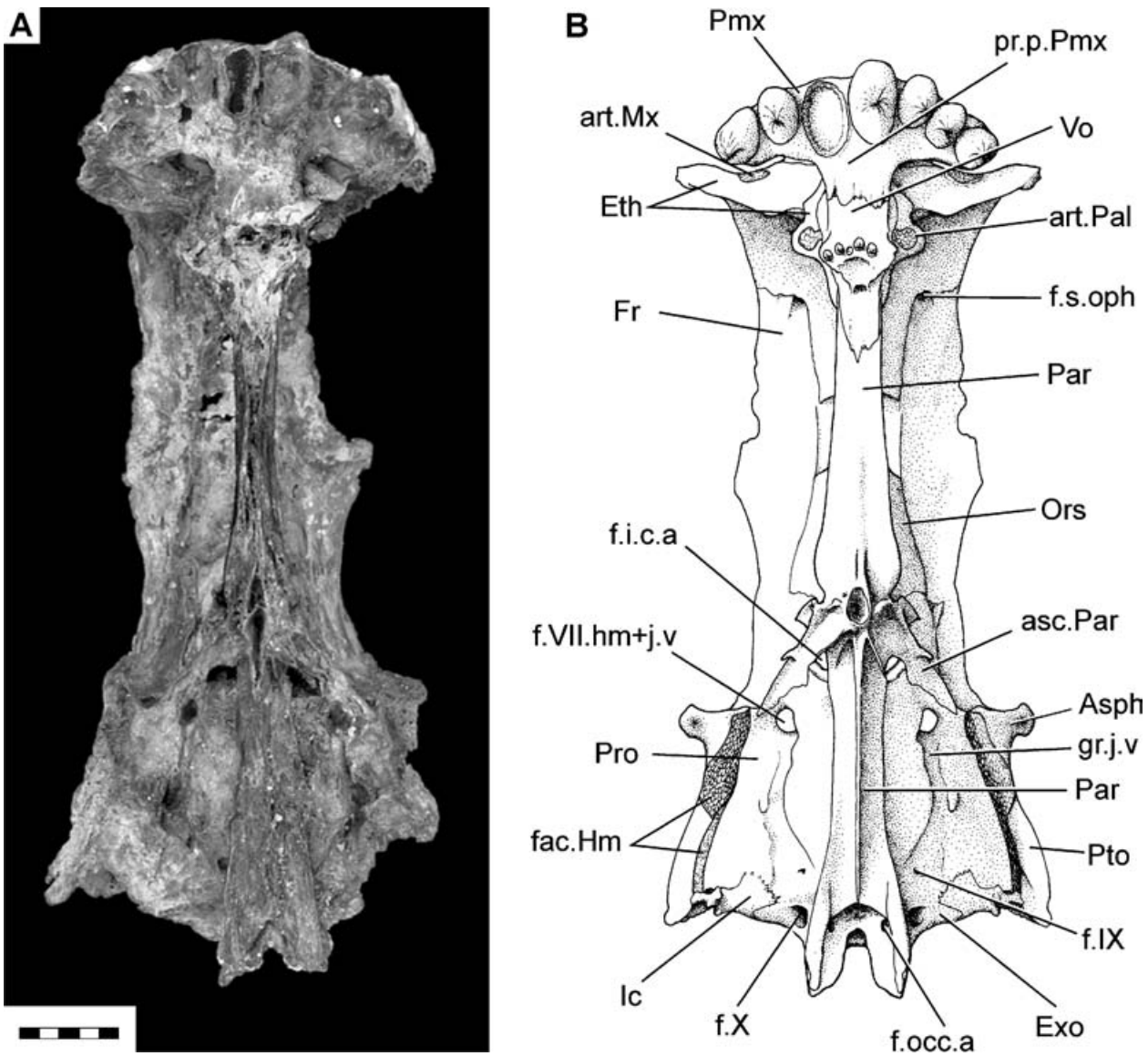


**Figure 5** †*Tomognathus mordax* Dixon, 1850. Ventral view of braincase. **A**, BMNH 49761; **B**, reconstruction based on BMNH 49761, 49765 and P.11799. Scale bar = 5 mm.

function. The posterior margin of the interorbital septum is formed, for the most part, by unfinished bone (Fig. 4A) and presumably passed into a cartilaginous interorbital septum. The ethmoid is pierced by two pairs of foramina that lie close to the mid line in the anterior orbital wall. The dorsalmost foramen is large, directed anteroventrally and marks the point of entry of the olfactory tract into the nasal capsule (Fig. 4: **f.I**). The ventralmost is much smaller, inclined anterodorsally and carried the infraorbital branch of the maxillary nerve (Fig. 4: **f.mx.V**) to innervate the ethmoid commissure within the rostral. The superficial ophthalmic (anterior dorsal lateral line nerve) pierces the rear wall of the nasal capsule close to the point where the ethmoid reaches the frontal (Figs 4A & 5: **f.s.oph**). The foramina are best seen in ventral view (Fig. 5).

The premaxilla (see Figs 3–6 & 15: **Pmx**) is very robust and, in all specimens examined, it is a median element. The tooth-bearing portion is bulbous and shows a roughened dorsal surface. The dorsal surface is developed as paired, thin, nasal processes (Fig. 4B: **n.pr.Pmx**). Each process is bifid and asymmetrical and has two dorsally directed limbs. The mesial limb is long, slender and curves dorsolaterally around the opening for the olfactory tract. The lateral limb is much stouter, but only reaches a short distance on the lateral side of the olfactory foramen. The premaxillary nasal process of †*Tomognathus* is unusual amongst halecomorphs in that it fails to completely surround the olfactory foramen. The point of divergence of the two limbs marks the point where the foramen for the infraorbital branch of the maxillary nerve pierces the ethmoid (Fig. 4B: **f.mx.V**). In ventral view the thickened part of the premaxilla is produced posteriorly as a median process (Fig. 5: **pr.p.Pmx**) that contacts the vomer through a complex, interdigitate suture. Such a process appears to be unique to †*Tomognathus*. The premaxilla carries seven or, more usually, eight very large, pointed teeth. Each tooth is hollow and laterally compressed, the mesially-placed

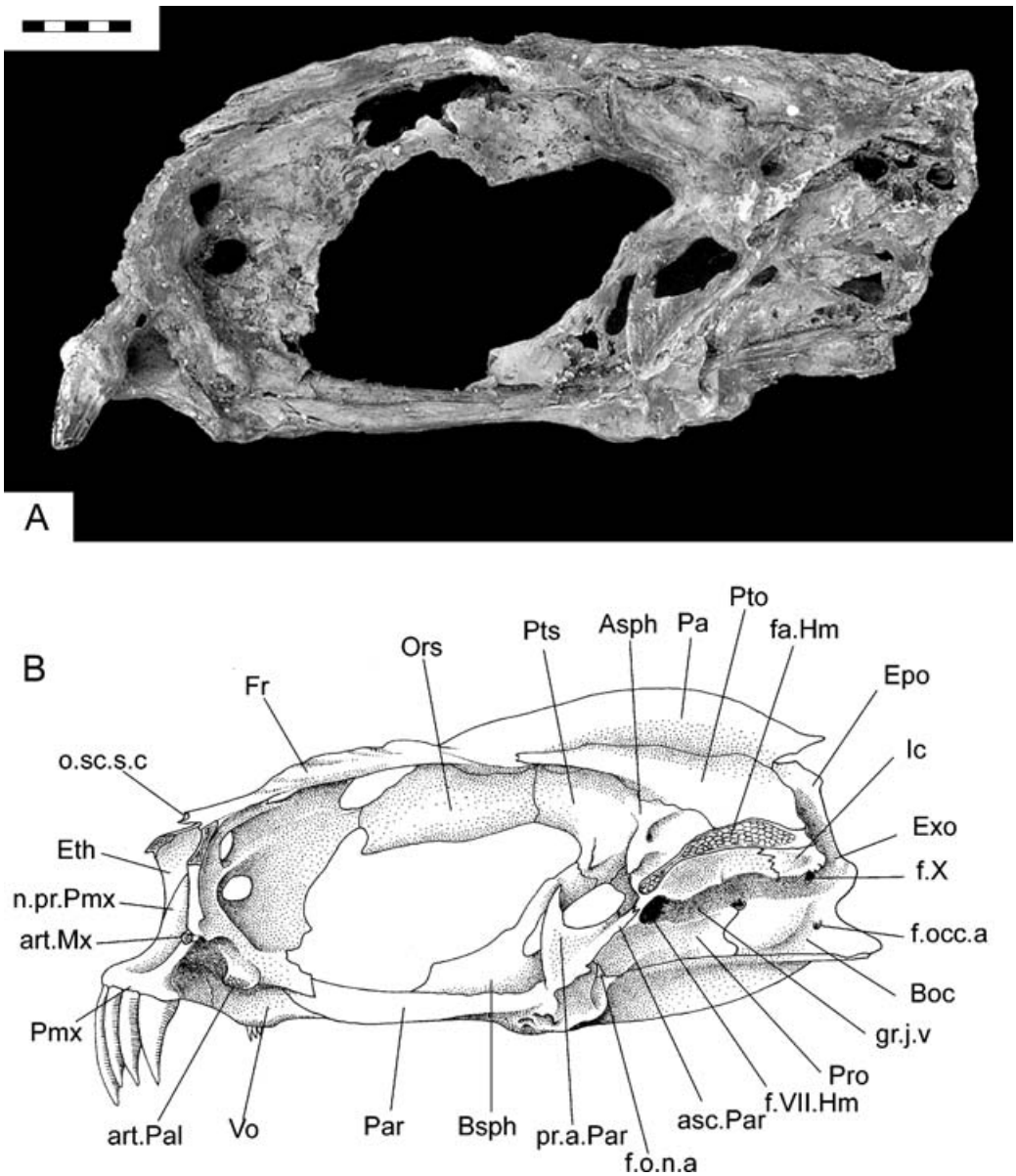


**Figure 6** †*Tomognathus mordax* Dixon, 1850. Lateral view of braincase. **A**, BMNH 49765; **B**, reconstruction based on BMNH 49761, 49765 and P.11799. Scale bar = 5 mm.

more so than the laterally-placed teeth (Fig. 5). Most of the enameled surface of each tooth is smooth but there may be a few minute ridges distally, immediately beneath the acrodin cap. The teeth are hollow with relatively thin walls. The vomer (Figs 4–6: **Vo**) is also unpaired. Anteriorly, it is sutured to the posterior process of the premaxilla. Posteriorly, there is a complex suture with the parasphenoid. The vomer carries four or five tiny teeth set in a transverse row.

The parasphenoid (see Figs 5, 6, 8 & 9: **Par**) is a bone of complex shape and very distinctive for †*Tomognathus*. It reaches from the anterior level of the orbit to the occiput. Beneath the orbit the parasphenoid is narrow and for most of its span it is rectangular in cross-section. Towards the rear of the orbit it becomes more complex with vertical and horizontal flanges intersecting each other (see Fig. 8B: **Par**). Beneath the otic region the parasphenoid has a strong median keel with paired, thin, dorsally directed wings that suture with the basiocciptal and prootic. Mid-way along the length of the parasphenoid the bone gives off a prominent ascending process on either side (see Figs 5, 6, 8B & 9: **asc.Par**). Each ascending process reaches dorsally to the level of the jugular canal and is sutured to the prootic through an oblique, deeply interdigitating suture. The anterior edge of the ascending process is produced as a thin, sickle-shaped process (see Figs 6, 8B & 9: **pr.a.Par**) that projects into the orbital cavity. This wing is unique to †*Tomognathus* and it is difficult to think of a function. It appears to be too thin for muscle attachment; it may have provided support for the eye capsule that must have been particularly large in this fish. At the confluence of the ascending process with the main body of the parasphenoid there is a notch for the efferent pseudospiracular artery. The base of the ascending process and the neighbouring part of the main body of the parasphenoid is deeply excavated by an antero-posteriorly orientated depression, presumably for

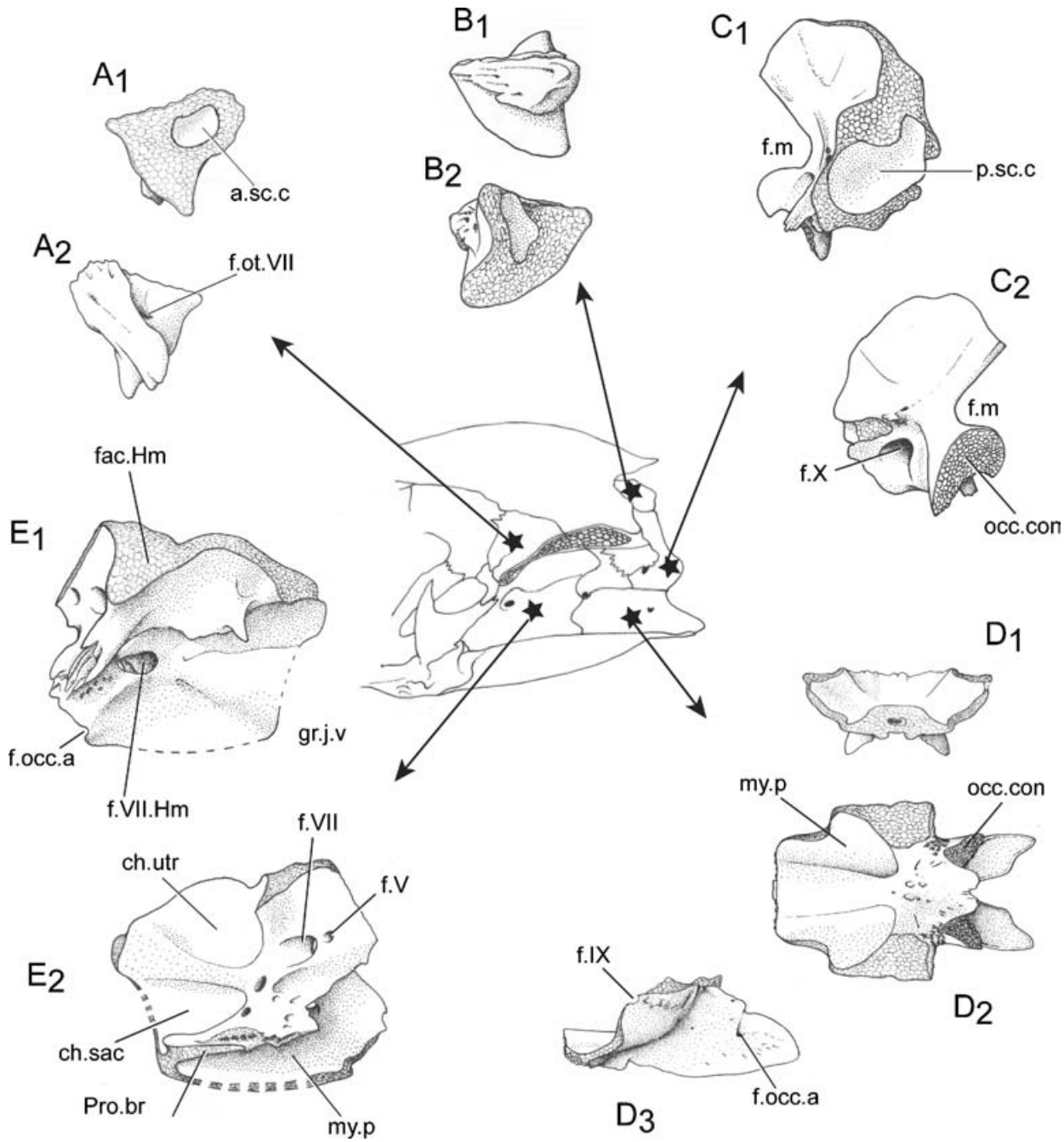


**Figure 7** †*Tomognathus mordax* Dixon, 1850. Isolated braincase ossiifications from BMNH P.1702 and 36172. Centre shows outline drawing locating individual ossifications within the braincase. **A**, BMNH 36172 – autosphenotic, $A_1$, internal face, $A_2$, left lateral face; **B**, BMNH 36172 – epioccipital, $B_1$, left lateral face, $B_2$, internal face; **C**, BMNH P.1702 – exoccipital of right side (reversed for ease of comparison) $C_1$, anterior face, $C_2$, posterior face; **D**, basioccpital, $D_1$, anterior face, $D_2$, dorsal face, $D_3$, left lateral face; **E**, BMNH P.1702 – prootic, $E_1$, left lateral face, $E_2$, internal face.

insertion of the dorsal gill arch muscles. The ventral surface of the parasphenoid at the level of the ascending process is marked by a deep median pit (Fig. 5B), sometimes (BMNH 49761) accompanied by prominent rugosities. There are no teeth on the parasphenoid.

The otic region of the braincase in the larger specimens shows very few sutures. However, two smaller specimens (BMNH P.1702 & 36172) were acid prepared and became disarticulated into component bones that demonstrate that the braincase presumably ossified as separate centres before becoming a consolidated unit in the adult stage. Figure 7 shows the separate elements and these are described here and are positioned on a schematic diagram of the braincase. The exoccipital (Figs 3, 5, 6, 7C & 8A: **Exo**) completely encloses the foramen magnum (Figs $7C_{1,2}$ & 8A: **f.m**). It also forms the dorsolateral aspect to the occipital condyle (Fig. $7C_2$: **occ.con**). Immediately anterior to the occipital condyle portion the large opening for the vagus nerve can be seen. The bone is excavated on the mesial side by the ampulla for the posterior semicircular canal (Fig. $7C_1$: **p.sc.c**), as well

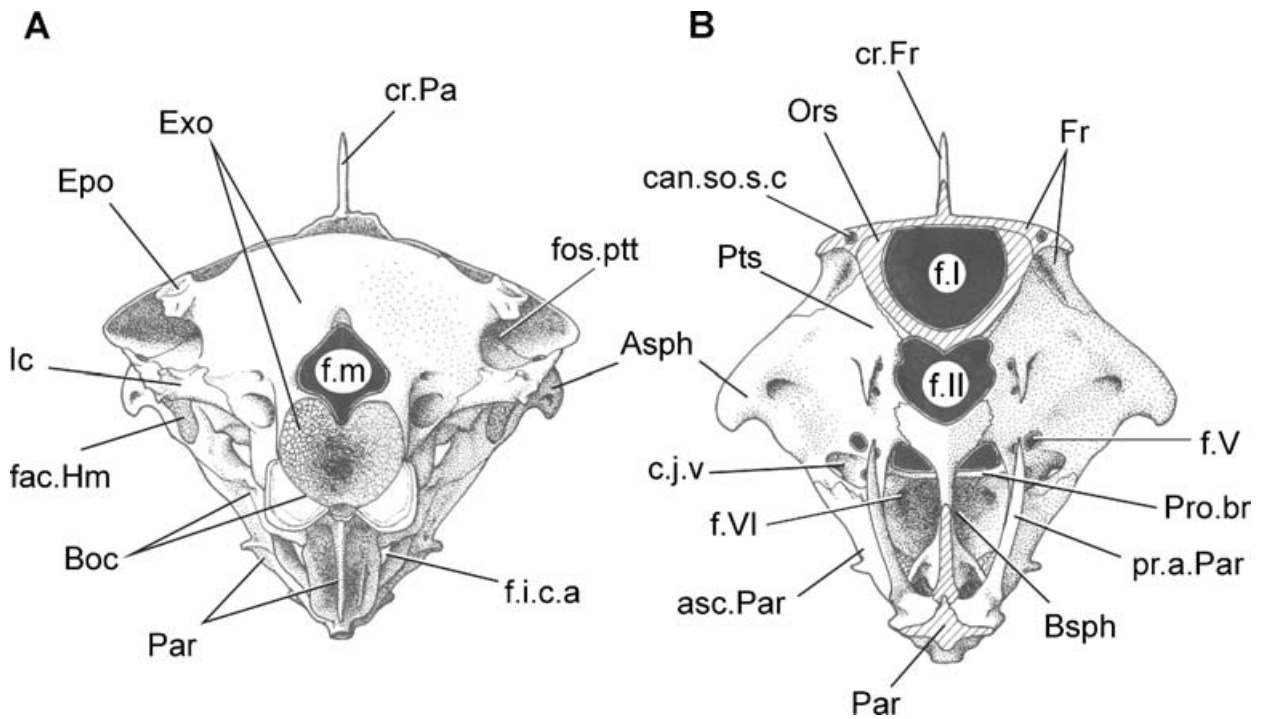


**Figure 8** †*Tomognathus mordax* Dixon, 1850. Reconstructions of **A**, posterior view of braincase, **B**, posterior orbital wall. Based mainly on BMNH 49761, 49765 and P.11799. Approximately × 4 natural size.

as the base of the tube that enclosed that semicircular canal. A small foramen for a spinal occipital nerve is seen piercing the exoccipital immediately posterior to the vagus foramen (Figs 5, 6 & 7$C_2$: **f.X**).

The epioccipital (Figs 3, 6, 7B & 8A: **Epo**) is small and bears a rugose surface, presumably for the attachment of the dorsal limb of the posttemporal, although this was not seen. The intercalar (Figs 5, 6 & 8A: **Ic**) is only seen in articulated braincases in our material and this may testify to its very thin membranous nature. The posterior surface is very rugose where it forms the ventral margin to the opening into the posttemporal fossa. This rugosity presumably received tendons linking the ventral limb of the posttemporal to the intercalar. The lateral face of the intercalar spread out over the exoccipital. We are uncertain if it reached the prootic as in *Amia* but the limited anterior extent (Fig. 5) suggests that it did not.

The basioccipital (Figs 3, 6, 7D & 8A: **Boc**) forms the lower half of the occipital condyle, which shows unfinished bone within the notochordal pit. This surface must have been lined with cartilage or the fibrous sheath of the notochord. In posterior view (Fig. 8A) the condyle is heart-shaped, the dorsal indentation being formed by the peculiar shape of the foramen magnum (Fig. 8A: **f.m**). The dorsal lobes of the heart-shape are formed by the paired exoccipitals (see above). The anterior end of the basioccipital is flared as it forms the posterior limits of the posterior myodome (Fig. 7$D_2$: **my.p**). Paired, thin outgrowths are developed posteriorly and each is pierced by a dorsally directed foramen. The membranous wings subtend an anteriorly directed pit for the insertion of the aortic ligament. The foramina are probably for the dorsal passage of paired occipital arteries (Fig. 7$D_3$: **f.occ.a**). A small notch in the dorsal margin of the basioccipital (Fig. 7$D_3$: **f.IX**) marks the position of exit of the glossopharyngeal. This foramen was probably closed by a matching edge on the exoccipital. There is no evidence of any centra having been incorporated into the occiput in †*Tomognathus*.

The prootic (Figs 5, 6 & 7E: **Pro**) lies anterior to the exoccipital. The dorsal edge of this bone forms the anterior part of the hyomandibular facet (Figs 6 & 7$E_1$: **fac.Hm**). On the lateral surface the prootic is marked by a deep, horizontal groove that carried the jugular vein (Figs 5, 6 & 7$E_1$: **gr.j.v**). In BMNH P.1702 there is a small overhanging process of bone mid-way along the length of the horizontal groove. This could not be identified in the larger braincases and its significance is unknown. At the anterior edge of the lateral surface the prootic shows a complex sutural surface for contact with the ascending process of the parasphenoid. Immediately behind this level both the posterior opening of the jugular canal as well as the foramen for the hyomandibular branch of the facial nerve (Figs 6 & 7$E_1$: **f.VII.Hm**) can be seen. The anteroventral angle of the prootic margin is notched for the passage of the orbitonasal artery. The anterior face of the prootic is small. It is sutured to the pterosphenoid and autosphenotic. Foramina for the exit of the trigeminal (Figs 7$E_2$ & 8B: **f.V**) and the palatine branch of the facial (Fig. 9: **f.VII.pal**) can be seen, as can the entrance to the jugular canal (Fig. 8B: **c.j.v**). The internal face of the prootic shows two large depressions within its posterior half, one above the other; the dorsal one is the utricular chamber (Fig. 7$E_2$: **ch.utr**) and the ventral one the saccular chamber (Fig. 7$E_2$: **ch.sac**). Beneath the latter the prootic bridge (Fig. 7$E_2$ & 8B: **Pro.br**) can be seen, delimiting the roof of the posterior myodome (Figs 7$E_2$ & 9: **my.p**). The posterior myodome is closed posteriorly but is very large, in keeping with the large orbit. The abducens entered the myodome well anterior to the prootic bridge.

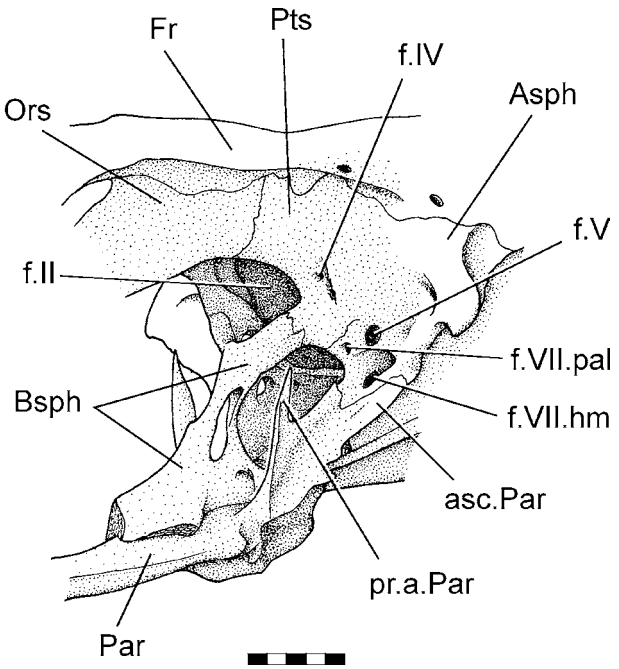


**Figure 9** †*Tomognathus mordax* Dixon, 1850. Reconstruction of orbital wall of otic region in oblique left anterolateral view. Based mainly on BMNH 49765. Scale bar = 5 mm.

The autosphenotic (Figs 3, 5, 6, 7A, 8 & 9: **Asph**) is small, pyramidal and with a rugose lateral process. The dorsal surface is penetrated by a foramen for the otic branch of the facial (Fig. $7A_2$: **f.ot.VII**) and the body of the bone is traversed by the tube for the anterior semicircular canal (Fig. $7A_1$: **a.sc.c**). The pterosphenoid (Figs 6, 8B & 9: **Pts**) is confined to the postorbital wall where it sutures with the autosphenotic, prootic, basisphenoid and the orbitosphenoid and forms part of the margins for the optic foramen and the anterior opening into the posterior myodome. The shape of the pterosphenoid is best seen in BMNH 49765 (Fig. 9). Two closely-spaced foramina pierce the bone for the passage of the oculomotor and trochlear nerves (Fig. 9: **f.IV**). The median orbitosphenoid (Figs 5, 6, 8B & 9: **Ors**) is large and reaches well forward in the roof of the orbit where it is sutured to the interorbital septum. The basisphenoid (Figs 6, 8B & 9: **Bsph**) is a complex bone. The dorsal part is 'Y'-shaped and the wings of the 'Y' suture with the pterosphenoids. The median pedicel of the basisphenoid is very stout and fenestrated. The ventral part of the basisphenoid is flared ventrolaterally and, with the parasphenoid, these form the walls of paired recesses that lie anteriorly and separately to the posterior myodome; the function of these recesses is unknown.

## Hyopalatine series

Elements of the hyopalatine series are seen in several specimens (BMNH 49766, 49768, P.4844, P.5675, P.5676, P.6460, P.9237 & BM B.9164) but the description below is based largely on two acid-prepared specimens (BMNH 49761 and 49765). The overall shape of the palate is very *Amia*-like, the relative sizes of the constituent bones being very similar, with a large metapterygoid and ectopterygoid and a small quadrate.

The hyomandibular (see Figs 10, 12 & 15: **Hm**) is thin, almost plate-like. The single articulatory head extends the length of the otic region. The opercular process (see Figs 10A & 12D: **pr.Op**) is ill-defined while the shaft is anteroposteriorly broad. With the skull in the resting position (mouth closed) the shaft would have been inclined only slightly posteriorly. The ventral end of the hyomandibular shaft ends in a narrow, elongate, open-ended surface (see Fig. 12D) indicating that, in life, there was a substantial cartilage end. The internal surface of the hyomandibular is perfectly smooth. It is pierced at the level of the opercular process by the foramen for the hyomandibular trunk of the facial nerve (Figs 10A & D: **f.VII.Hm**). The external surface of the hyomandibular is marked by a longitudinal ridge, although this is not particularly well developed. The hyomandibular branch of the facial nerve exits its path through the bone immediately behind this ridge. The anterior edge of the shaft is produced as a thin wing of bone (usually fractured in specimens). The preopercle fits closely against the posterior margin of the hyomandibular ridge (it is displaced anteriorly in Fig. 10B). The anterior ceratohyal is only partly known as a short, posteriorly expanded section (Fig. 10A: **Ch.a**). We have not seen a posterior ceratohyal.

At the ventral end of the hyomandibular lies the symplectic (see Figs 10A, B & 12D: **Sy**). This is a complex-shaped bone. The lateral edge is formed by a tubular portion that is open dorsally and presumably passed to cartilage contiguous with cartilage at the ventral end of the hyomandibular. The mutual relationships between the symplectic and hyomandibular are, therefore, assumed to be as in *Amia* (Grande & Bemis 1998: fig. 48). The posterior edge of the symplectic is produced dorsally beyond the open end and formed a closed process (see Fig. 12D: **pr.Sy**). The ventral end of the symplectic is developed as a condylar surface and this area is sutured tightly with the quadrate such that both elements, quadrate and symplectic, form a double condyle (see Fig. 12D). Therefore, although both quadrate and symplectic take part in the jaw joint the two articulations form a single functional unit. This is similar to that in most halecomorphs. In *Amia calva* and, possibly, other species of *Amia*, the two articulations are well separated (Grande & Bemis 1998: fig. 49C). The quadrate (see Figs 10, 12D & 15: **Qu**) is relatively small, triangular and bears a small articular condyle. The dorsal edge of the quadrate is unfinished and presumably passed into the palatoquadrate cartilage.

The metapterygoid (see Figs 10 & 15: **Mpt**) is formed of thin bone and the edges are often broken. It is longer than deep and overlaps part of the hyomandibular as well as the entopterygoid. The dorsal margin is produced as a small process (see Figs 10C & 15) midway along its length. Grande & Bemis (1998: 85) describe a similar process in *Amia calva*. In *Amia calva* the process is associated with a notch, through which passes the maxillary and mandibular branches of the trigeminal nerve. †*Tomognathus* lacks the notch but we assume that the process had similar topological relationships with the trigeminal nerve. There are no teeth associated with the metapterygoid (cf. *Amia calva*, Grande & Bemis 1998: fig. 49B).

The entopterygoid (see Figs 10C, D & 15: **Enpt**) is large, wide posteriorly and narrows to a point anteriorly. The bone is dorsally concave, ventrally convex and carries a distinct central patch of many, tiny, villiform teeth upon the oral surface (Figs 10D: **tp.Enpt**). The entopteryoid is sutured with

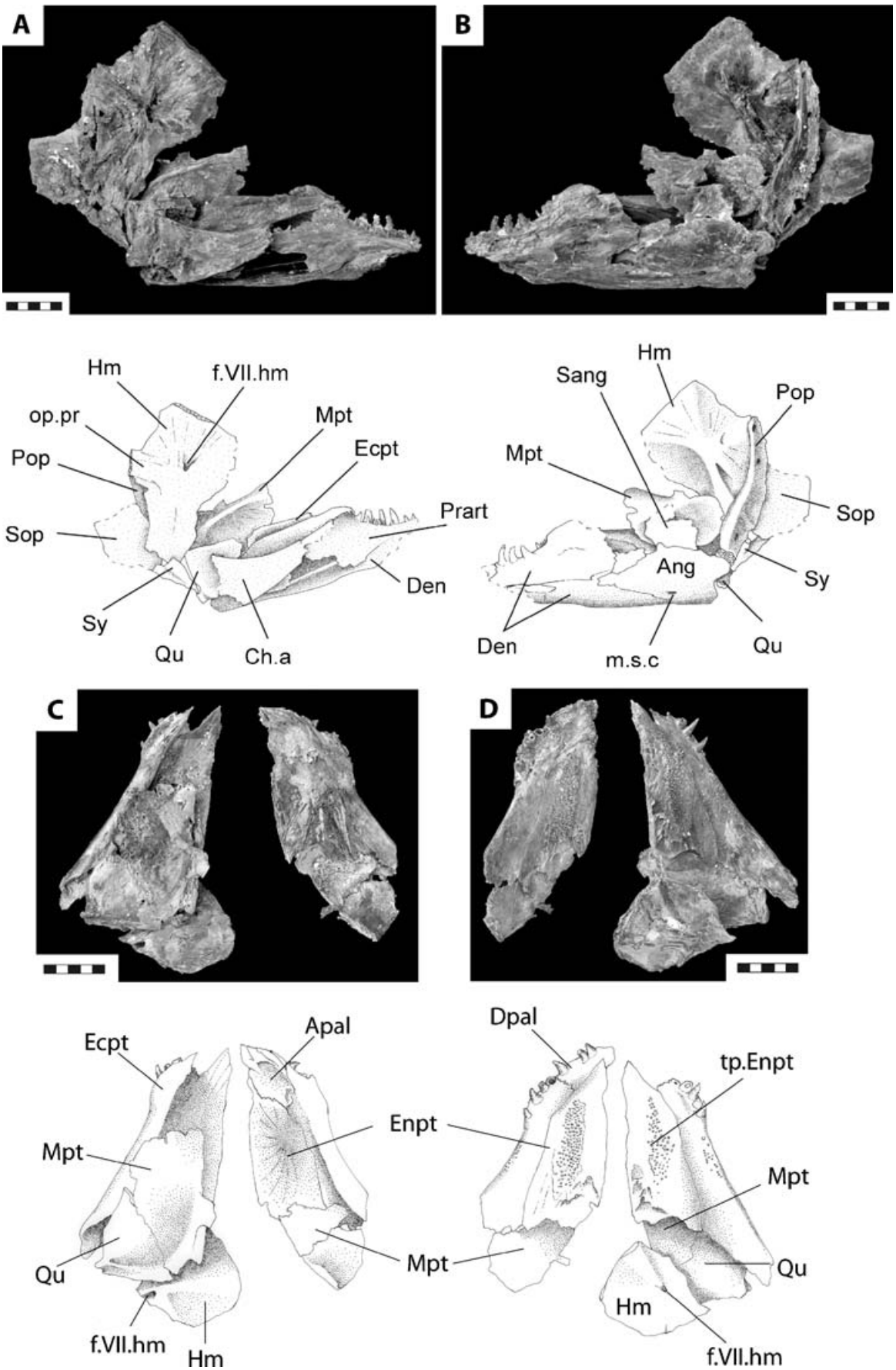


**Figure 10** †*Tomognathus mordax* Dixon, 1850. Hyoid arch and palate. **A**, BMNH P.66297 mesial view of left hyoid arch, palate and lower jaw with interpretive drawing; **B**, BMNH P.66297 lateral view and interpretive drawing; **C**, BMNH 49765 isolated palatal bones in dorsal view with interpretive drawing; **D**, BMNH 49765 ventral view with interpretive drawing. Scale bars = 5 mm.

the ectopterygoid laterally and the dermopalatine anteriorly. The ectopterygoid (see Figs 10A, C & 15: **Ecpt**) is very robust. Posteriorly, it is slightly expanded and grooved along the dorsal (mesial) margin. Part of the quadrate lies in this groove. The ectopterygoid dentition consists of four large, conical and slightly recurved teeth situated near the anterior end and lying in continuity with the palatine teeth. Behind this level there is a small patch of tiny teeth, comparable in size with those upon the entopterygoid (Fig. 10D).

The palatine consists of separate auto- and dermopalatine components. The dermopalatine (Fig. 10D: **Dpal**) is small, triangular and sutured to the ectopterygoid and entopterygoid. Three large, conical and slightly recurved teeth are present in BMNH 49765 (right side). †*Tomognathus* is very unusual amongst halecomorphs in showing a single dermopalatine (most have two). The autopalatine (Fig. 10C: **Apal**) is present as a thin perichondral shell of bone plastered onto the dorsal surface of the dermopalatine. The posterior margin of the autopalatine is very irregular and it is probable that it passed into cartilage which must also have formed the core of the autopalatine. In Recent teleosts the autopalatine is often the last of the palatal bones to ossify within the palatoquadrate cartilage and it often fails to ossify at all in many fishes. Therefore, the slight ossification of this element in †*Tomognathus* is not unusual.

## Maxilla and supramaxilla

The maxilla (see Figs 11 & 15: **Mx**) is a slender element with a narrow inturned head and a posteriorly expanded blade. There is a single supramaxilla (see Fig. 15: **smx**). No single specimen shows a perfectly preserved upper jaw: therefore well preserved elements are taken from three specimens (Fig. 11). The outline of the maxilla is best preserved in BMNH P.3849, Fig 11B). Here the true posterior margin can be seen. The shape of the posterior margin is of some importance in halecomorphs and in this feature †*Tomognathus* most closely resembles †*Ionoscopus*, †*Amiopsis* and †*Solnhofenamia*, rather than members of the Amiista, in which the posterior margin is deeply notched (see Grande & Bemis 1998: fig. 243 for comparative outlines). The maxillary teeth are, on average, substantially smaller than the premaxillary and dentary teeth. This differentiation is seen in members of the Amioidea and contrasts with the situation in other halecomorphs, in which the teeth are of approximately the same size. There are 26–37 teeth along the oral margin of the maxilla. The dentition is best displayed in SM B.9164 (34 teeth), which shows a gradation in tooth size along the margin (Fig. 11A). The anteriormost teeth are nearly four times as long as the posterior teeth. In the largest specimens at our disposal (BMNH P.20122) the size differentiation between anteriormost and posteriormost teeth is considerably less (Fig. 11C). We do not know if this is individual variation or a growth phenomenon. All teeth bear acrodin caps and the larger anterior teeth are ridged, like their counterparts on the premaxilla and the lower jaw. The head of the maxilla is strongly inturned as a rod-like process and this would have articulated with the anteriorly directed process on the ethmoid (see Figs 4B, 5 & 6: **art.Mx**). The ornament on the maxilla consists of irregular shaped tubercles located posteriorly. The supramaxilla is rarely preserved, suggesting that it was loosely associated with the maxilla. It is best seen in BMNH P.20122 (Fig. 11C). The shape of the supramaxilla mirrors that of the maxilla and it is about half the length of the maxilla.

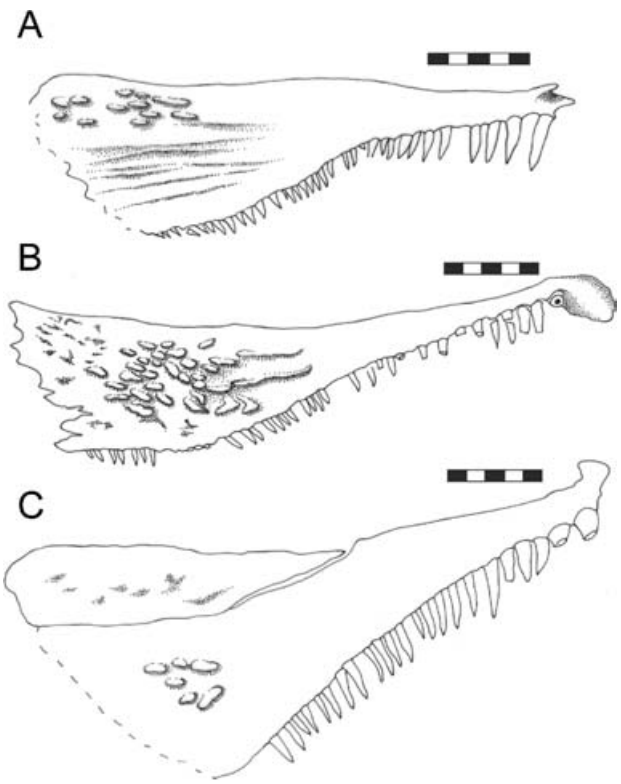


**Figure 11** †*Tomognathus mordax* Dixon, 1850. Maxilla and supramaxilla of right side – camera lucida drawings. **A**, SM B.9164; **B**, BMNH P.3849; **C**, BMNH P.20122. Scale bars = 5 mm.

## Lower jaw

The structure of the lower jaw is one of the most obvious reasons to question Woodward's view that †*Tomognathus* is a stomiiform. The lower jaw shows a coronoid, prearticular and surangular – all bones that are absent and presumed lost in teleosts (although Nelson (1973: 338) admitted the possibility that coronoids had fused with the dentary and the surangular with the angular).

The lower jaw is shallow anteriorly, it deepens to a prominent coronoid process and ends posteriorly in a robust condylar area. The relative proportions of the dentary toothed area to the total length of the jaw is 37–40% and this is more like the proportions seen in parasemionotids and amioids than in caturids, in which the toothed area extends for about 60% of the total jaw length.

The outer surface of the mandible is formed by the dentary, angular and surangular. From a shallow symphysis the dentary (see Figs 10A, B, 12A–C & 15: **Den**) deepens considerably and contacts the angular through an interdigitate suture. There is a single row of nine or 10 teeth along the oral margin. Those anteriorly are substantially larger that the posterior teeth and the largest are comparable in size to the premaxillary teeth and, like those teeth, they show anteroposteriorly compressed bases. The size differentiation between anterior and posterior teeth is variable between individuals, as is the position of the largest tooth (which is either the third

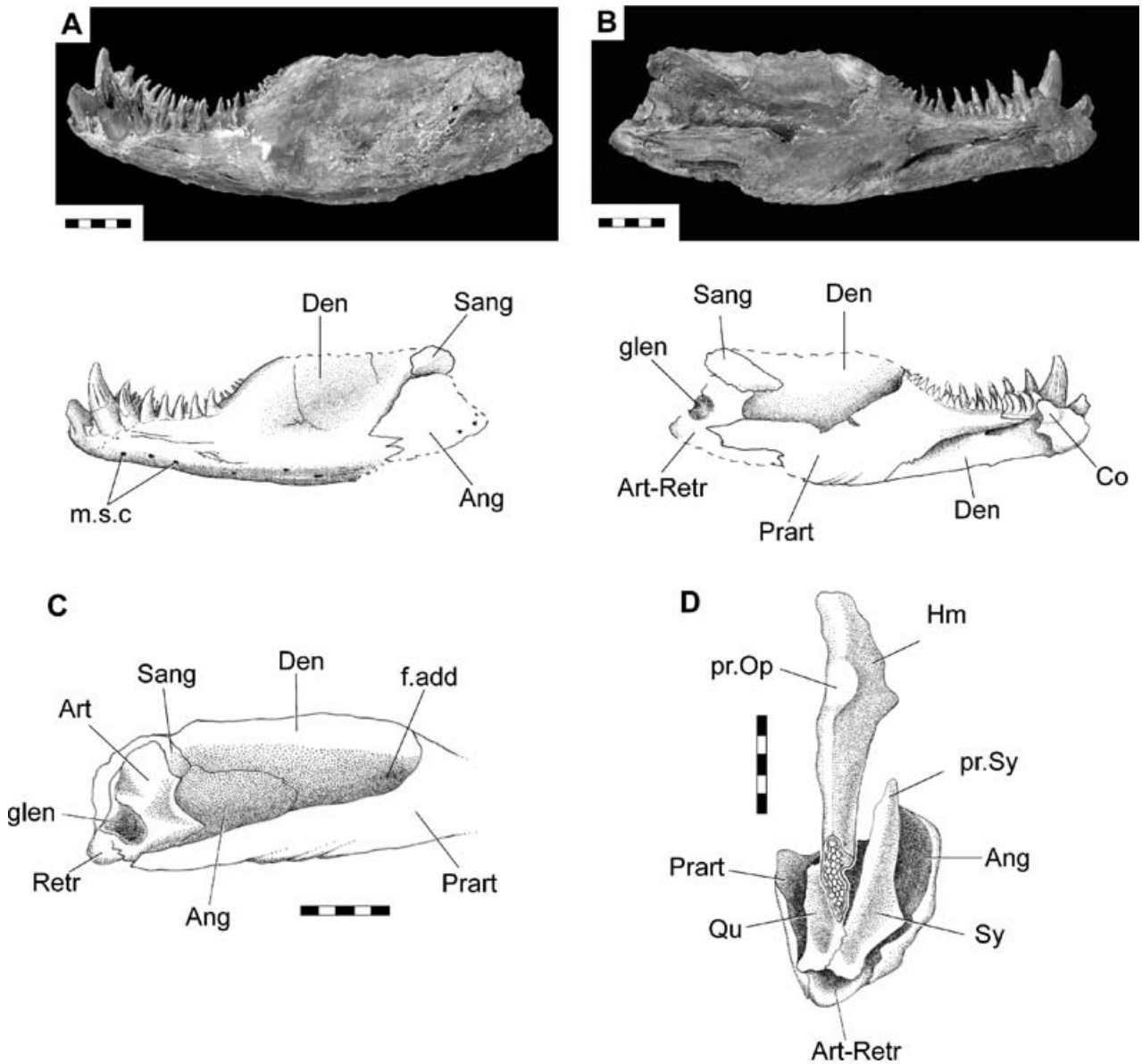


**Figure 12** †*Tomognathus mordax* Dixon, 1850. Lower jaw. **A**, lateral face as preserved in BMNH 49765 with interpretive drawing; **B**, mesial face with interpretive drawing; **C**, mesial view posterior end of jaw as preserved in BMNH 49761 to show articular–retroarticular; **D**, posterior view of jaw joint of right side as preserved in BMNH 49761. Scale bars = 5 mm.

or fourth in the series). In general, the differentiation in size is greater in larger specimens than in smaller specimens. The larger teeth show bases ensheathed in a thin layer of bone that extends up to about one-third of their height. These teeth also show a ridged surface in larger specimens.

The angular (see Figs 10B, 12A, C, D & 15: **Ang**) is relatively small, composing less than a quarter of the lateral surface area. The surangular (see Figs 10B, 12A–C & 15: **Sang**) is very small and is partially overlapped by both the angular and the dentary so that is appears larger on the mesial face of the jaw (Fig. 12B). The mandibular sensory canal enters the jaw at the extreme posterior end of the angular and traverses the angular and dentary, opening by a series of round pores (Fig. 12A: **m.s.c**). In one specimen (BMNH P.11799) the outer surface of the left dentary is broken beneath the third and fourth tooth. This break reveals a large cavity that is an anteriorly expanded portion of the mandibular sensory canal. Such an expansion may be manifest in intact jaws where the anterior sensory pores tend to get out of line (see also *Amia calva*, Grande & Bemis 1998: fig. 46).

The mesial surface of the jaw shows a coronoid, prearticular and articular–retroarticular. The articular–retroarticular (Figs 12B & D: **Art-Retr**) is excavated by a glenoid fossa for the jaw articulation (Fig. 12C: **glen**). One specimen (BMNH 49761, Fig. 12C) shows a partial suture between the articular and retroarticular components and this suggests that the latter is excluded from any involvement with the jaw articulation.

The prearticular (Figs 10A & 12B–D: **Prart**) is a long element, sutured to the dentary and, with that bone, forms the adductor fossa (Fig. 10B & C: **f.add**). Dentition is confined

to a single row of teeth. In others, an outer row of enlarged teeth is accompanied by a shagreen of villiform teeth spread over the oral surface (e.g. see *Amia calva*, Grande & Bemis 1998: fig. 45). The prearticular extends further forward than in other halecomorphs and covers territory occupied by separate coronoids in other halecomorphs. In †*Tomognathus* there is a single coronoid (Fig. 12B: **Co**) lying mesial to the enlarged teeth upon the dentary. This coronoid carries a single row of five or six incurved teeth that lie in series with the row upon the prearticular. †*Tomognathus* is unique in having only a single coronoid; most other halecomorphs have three to five. †*Tomognathus* is also unusual in having only a single row of coronoid teeth: however, this condition is also seen in †*Calamopleurus cylindricus* (Grande & Bemis 1998: fig. 310).

## Circumorbitals, nasals and rostral ossicles

All of the circumorbital bones are very delicate and usually poorly preserved. The bones surrounding the eye are very reduced; there is no suborbital or supraorbitals and a sclerotic ossicle is missing. The dermosphenotic (see Fig. 15: **Dsph**) is a characteristic 'T'-shaped bone and this is located well anterior to the level of the autosphenotic spine (BMNH P.4844, SM B.9164). The stem of the bone is tubular and little larger than the contained canal. The head is expanded and is pierced along its dorsal margin for the infraorbital canal that, at this level, lies opposite the anterior opening of the otic sensory canal. The dermosphenotic lies completely free from the skull roof and this is an unusual feature seen only in parasemiontids and †*Calamopleurus cylindricus* among halecomorphs. Grande & Bemis (1998) consider a free dermosphenotic to be a plesiomorphic character at the halecomorph level but derived for †*Calamopleurus cylindricus*, which is nested deep within halecomorphs in which the dermosphenotic is an integral part of the skull roof. Its status in †*Tomognathus* is similarly revealed by optimisation. Two more tubular infraorbitals (see Fig. 15: **Inf** and **Inf$_1$**) can be seen reaching to mid-orbital level along the ventral rim. Infraorbital 1 (lachrymal) consists of a posterior tubular portion that expands to a rounded and plate-like anterior head (BMNH 49761). The tubular portion is perforated by two or three pores leading from the infraorbital canal and this canal leaves infraorbital 1 through an anteroventrally placed opening.

The rostral, antorbitals and nasals are best seen in BMNH 49761. The antorbital (see Figs 13 & 15: **Ao**) is a small, curved and tubular bone, perforated by four dorsal openings leading from the ethmoid commissure. The rostral (see Figs 13 & 15: **Ros**) is a median, shallow 'V'-shaped bone carrying the ethmoid commissure across the mid line from the antorbital. The nasal (see Figs 13 & 15: **Na**) is a broad plate produced posteriorly as a short tube. The nasal contacts its antimere anteriorly but the length of contact is very short. A small notch in the anterior margin is probably the position of the anterior nares (Fig. 13: **nos.a**). The supraorbital sensory canal (Fig.13: **so.s.c**) runs across the nasal in a raised tube and opens through a terminal pore close to the anterior margin. It is clear that, in life, the nasals failed to completely cover the nasal sacs (unlike the condition in most halecomorphs where the nasals are relatively larger and united in the midline throughout their length). The relative size, shape and nature of mutual contact of the nasals is most like

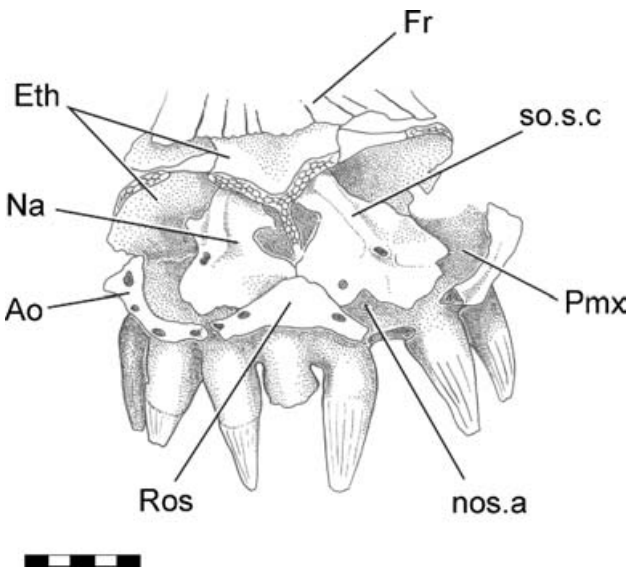


**Figure 13** †*Tomognathus mordax* Dixon, 1850. Snout ossicles. Anterior view of BMNH 49761 to show position and shape of nasals, antorbital and rostral ossicle. Scale bar = 5 mm.

those of †*Solnhofenamia elongata* amongst halecomorphs (Grande & Bemis 1998: fig. 333).

## Opercular series, branchiostegals and gular

A preopercle, opercle, subopercle and interopercle make up the opercular series. The preopercle (see Figs 10A, B & 15: **Pop**) is narrow, anteriorly curved and slightly expanded in its ventral half. The overall shape resembles that of most halecomorphs (Grande & Bemis 1998: 242). The opercle (see Fig. 15: **Op**) is equidimensional with broadly rounded dorsal and posterior margins. The ventral margin is finely indented. The facet for the opercular process of the hyomandibular is poorly defined. The subopercle (see Fig. 15: **Sop**) is nearly as large as the opercle and the rounded posterior and ventral margins continue the contours of the opercle. Both opercle and subopercle are ornamented with prominent ganoin covered tubercles and these are much better developed in larger individuals. There is a small, triangular interopercle (Fig. 15: **Iop**) that lies in series with the subopercle: it differs from the teleost condition where the interopercle is not only much larger but is also almost totally overlapped by the preopercle and subopercle. The interopercle is unornamented. The branchiostegal series is very poorly known. Both BMNH 39050 and P.65662 show evidence of at least four branchiostegal rays but their shapes are not completely known. In BMNH P.65662 the anterior three are very slender and filament-like (see Fig. 15: **Br.r**). The most posterior is completely different in being very broad, thin and showing a well developed and deepened articulatory head. Grande & Bemis (1998: 97) accepted earlier suggestions that this branchiostegal in amiids be termed a branchiopercle because it has a truncated head and, in *Amia calva*, is associated with a ligament connecting it to the lower jaw. We use this term here (see Fig. 15: **Brp**).

The median gular (Fig. 14) is very much like that of †*Calamopleurus*. It is fan-shaped with a broad flared posterior margin. Towards the posterior end there are radiating

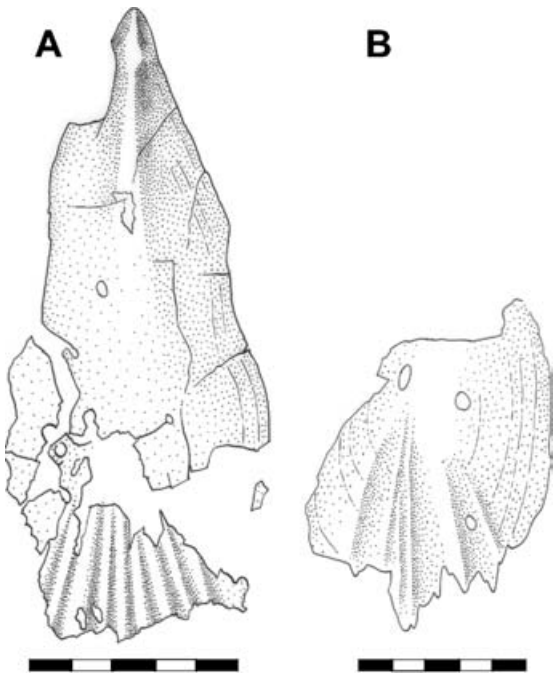


**Figure 14** †*Tomognathus mordax* Dixon, 1850. Gular plate – camera lucida drawings. **A**, SM B.9161; **B**, BMNH 49765. Scale bars = 5 mm.

ridges and these end in a pectinated margin (BM 016968 and BMNH 49765: Fig. 14B). At the anterior end of the gular there is a short median crest. This is similar to that in †*Calamopleurus africanus* (Forey & Grande 1998: fig. 6B) but unlike the gular of †*Calamopleurus cylindricus* in which there is no crest. The surface of the gular is ornamented with a few scattered tubercles and growth lines may also be seen.

## Postcranial skeleton

Very little is known about the postcranial skeleton of †*Tomognathus* and the incomplete restoration shown in Fig. 19 must be regarded as tentative. The outline shapes of the fins given in that figure are based on those in *Amia calva* with the justification that this is the only appropriate modern template for this taxon. In the data matrix such restoration is not used as a basis for coding characters. Four specimens only show parts of the postcranial skeleton (BMNH P.10632, P.1701, P.20122 and BM B.9164). BMNH P.10632 (Fig. 17) is the only specimen suggesting proportions of the body and relative positions of the fins and this is used for such parameters in Fig. 19.

The vertebral column is virtually unknown. No clear evidence of centra is known. In BMNH P.10632 two small patches of endochondral bone are seen above the anal fin and these may be remnants of centra, but little else can be said. In the anterior part of the body of BMNH P.10632 and P.1701 several ribs can be seen. These are very thin, straight, with simple proximal heads. They are short in comparison with the restored depth of the body. As such they resemble the ribs of *Amia*. BMNH P.10632 also shows a few scattered neural arches and spines and these, like the ribs, are very slender. At the posterior end of the column in this same specimen there are three endochondral elements interpreted here as hypurals.

Parts of the pectoral girdle and fin are seen in all four specimens where, collectively, the supracleithrum, cleithrum, scapulocoracoid and pectoral fin rays are partly known. The supracleithrum is relatively large (as deep as the operculum) as it is in all halecomorphs, and it is distinctively triangular in shape. Anterodorsally the supracleithrum narrows to a point. In BMNH P.10632, P.1701 and BM B.9164 the supracleithrum shows growth lines, eight in the first and last specimens and at least 10 in the other. The supracleithrum in BMNH P.20122 is largely covered by the operculum, but a few growth lines may be seen here also. The cleithrum (Fig. 16: **Cle**) is very imperfectly preserved in BMNH P.1701. The dorsal end is much expanded and there is a broad branchial lamina. The ventral end is imperfectly preserved. This specimen also shows a small portion of the scapulocoracoid (see Fig. 16: **Sca.cor**), but the details are too imperfect to allow further comment. The bases of at least 12 pectoral fin rays are preserved in BMNH P.1701 and P.20122. Some of the rays in BMNH P.20122 show multiple branching and close segmentation.

The pelvic fin is unknown. Two small portions of endochondral bone preserved midway along the body in BMNH P.10632 (see Fig. 17) are probably the dorsally displaced remains of pelvic bones. Each has a head, a constricted waist and an anteriorly flared lamina, as in the pelvic bones of *Amia calva*.

Some elements of both dorsal and anal fins can be seen in BMNH P.20122 and P.10632. The dorsal fin is best preserved in BMNH P.20122 (see Fig. 18), although neither its height nor its true length is known. The fin begins immediately behind the head (BMNH P.20122). The posterior limit is seen in BMNH P.10632 where its stops a short distance from the caudal fin. BMNH P.20122 shows that the fin contained at least 42 rays. The fact that the posteriormost rays are very small suggests that this figure is a reasonable estimate for the real count in life. Some of the anterior fin rays are relatively large (e.g. the seventh, as preserved, is almost as long as the length of the braincase) and this probably means that the fin is deeper anteriorly than posteriorly. It has been restored this way in Fig. 19. It thus differs from the true 'bowfin' of *Amia*, which is equally deep throughout its length or even slightly deeper posteriorly than anteriorly. All of the fin rays are paired and, as preserved, are unbranched. However, it is very likely that, in life, they were distally branched since the preserved portion of each ray is equidimensional throughout its length. It is significant that in *Amia calva* the branching of the dorsal fin rays is confined to the distal quarter of each ray (Grande & Bemis 1998: fig. 84). Segmentation can be seen in some of the rays. The anal fin is very poorly preserved in BMNH P.10632 where the bases of eight fin rays (two as impression only) can be seen. No segmentation or branching can be seen but this is probably the result of incomplete preservation.

Only a few remains of the caudal fin rays can be seen (BMNH P.10632). Each of these is very closely segmented, each segment being wider than long, and finely branched. The tail has been outlined in Fig. 19 after the tail shape in *Amia calva*. The true shape is unknown and it could be square-cut, more like that of *Amiopsis* or *Calamopleurus*. However, it is unlikely to have been forked since the disposition of the rays remaining in BMNH P.10632 show no evident break between upper and lower lobes.

The squamation is problematic. The body appears to be naked, except for a few stud-like elements found scattered near the tail of BMNH P.10632 (Fig. 20). We presume that

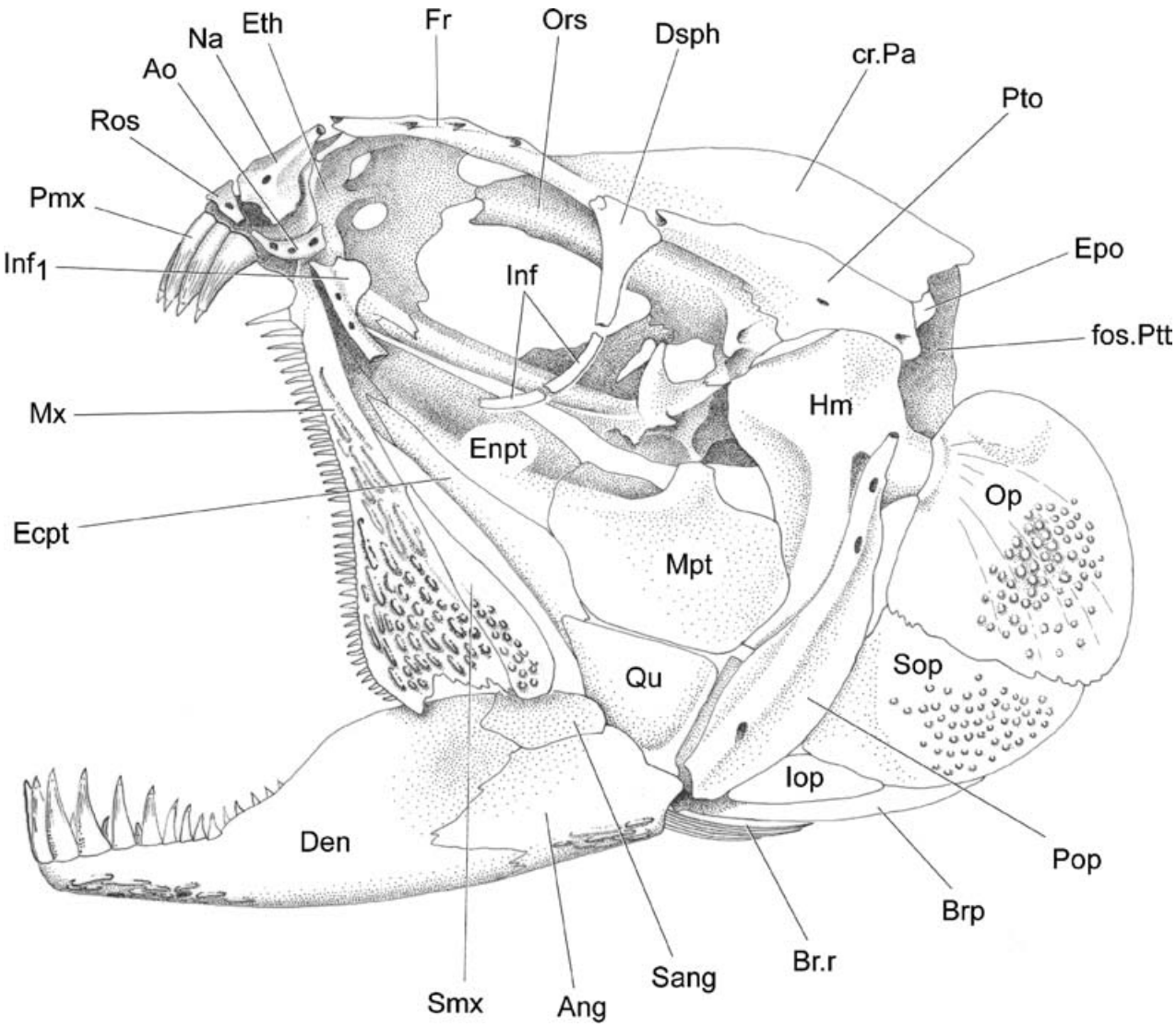


**Figure 15** †*Tomognathus mordax* Dixon, 1850. Reconstruction of head in left lateral view.

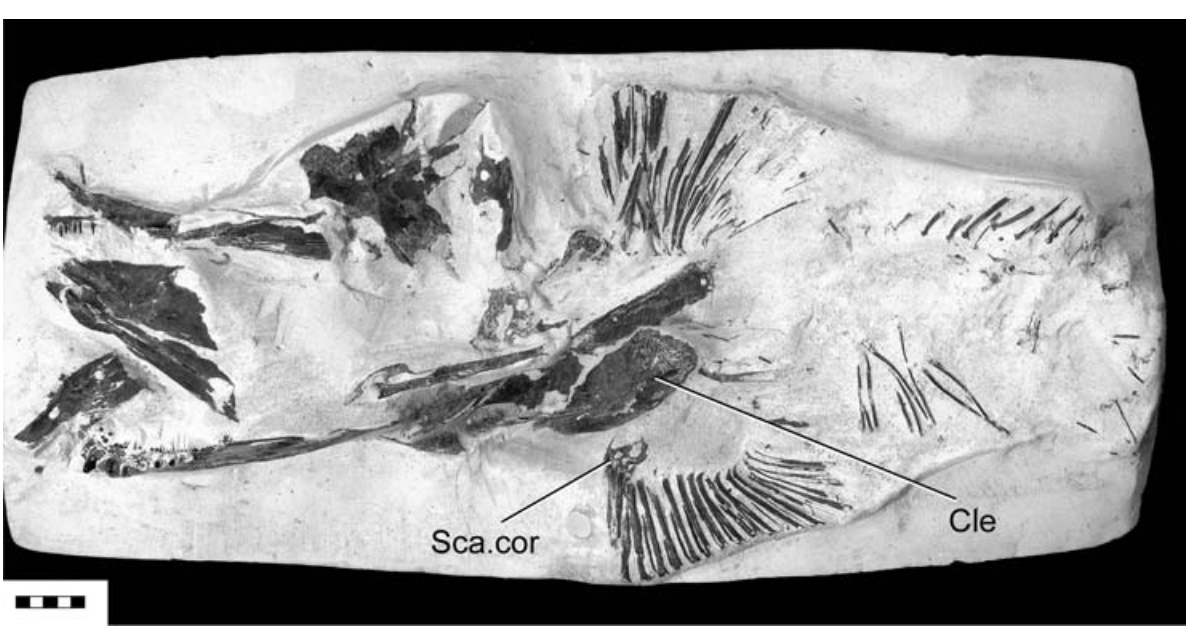


**Figure 16** †*Tomognathus mordax* Dixon, 1850. BMNH P.1701 showing partly preserved pectoral girdle and fin. Scale bar = 5 mm.

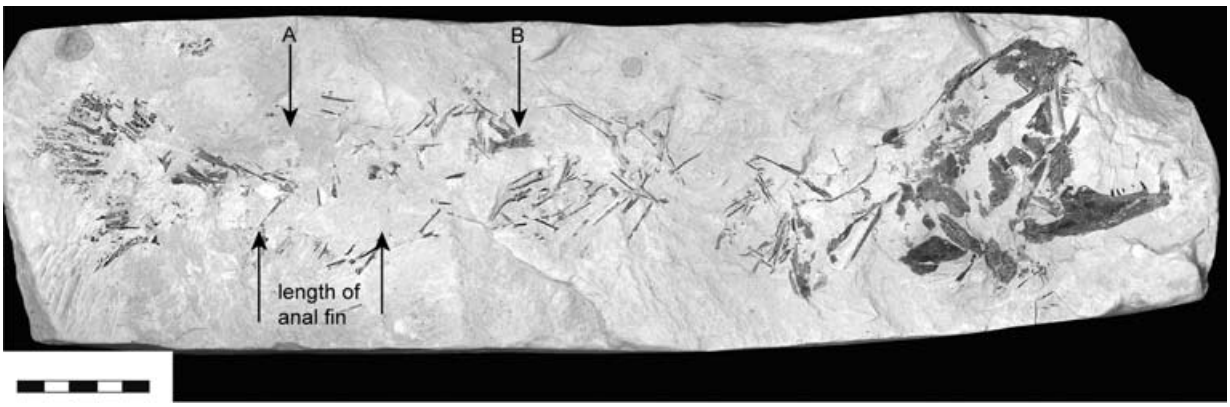


**Figure 17** †*Tomognathus mordax* Dixon, 1850. BMNH P.10632. Entire but incompletely preserved fish. This specimen is used for the proportions of the body in the reconstruction. The positions of the posterior ray of the dorsal fin is marked by arrow A, and possible pelvic bones by arrow B. Scale bar = 20 mm.

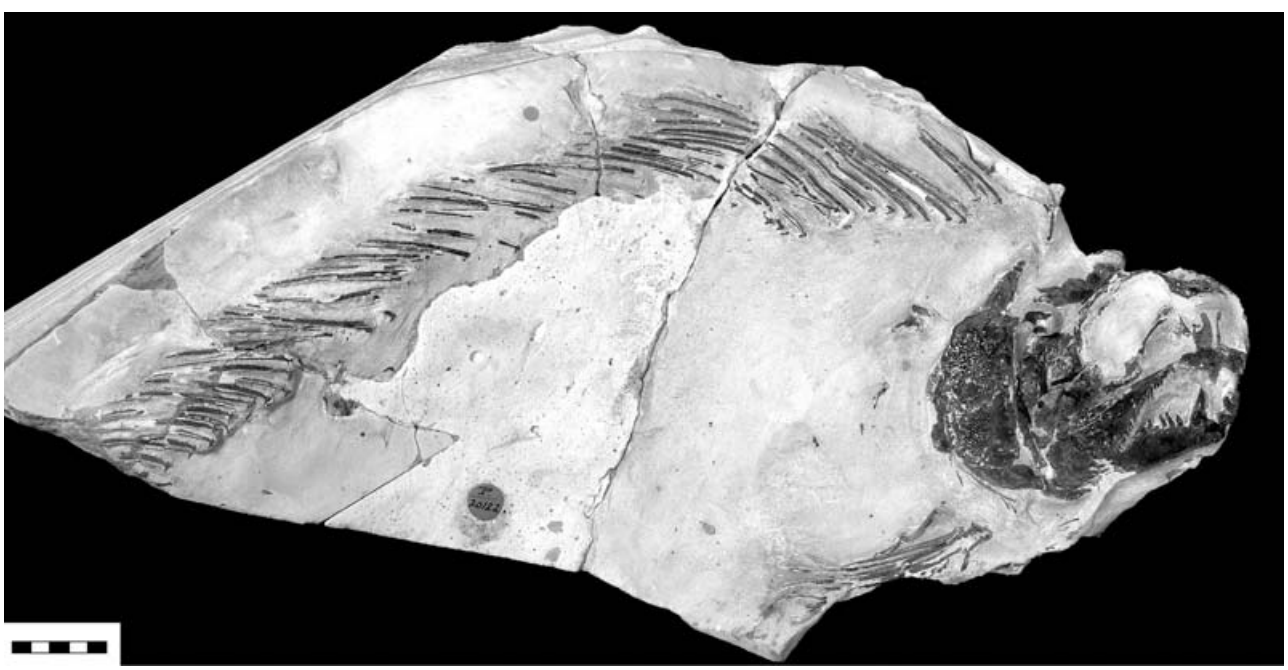

**Figure 18** †*Tomognathus mordax* Dixon, 1850. BMNH P.20122, a large specimen showing much of the dorsal fin. Scale bar = 20 mm.

they do belong with †*Tomognathus*. Each of these elements is approximately rhomboidal with a bony base and enameloid surface.

## Phylogenetic relationships

There are five reasons to believe that †*Tomognathus* belongs to the Subdivision Halecomorphi and that it is more closely related to *Amia* than to modern teleosts: the presence of a double jaw joint where the symplectic as well as the quadrate is involved with the jaw joint, the concave shape of the posterior margin of the maxilla, a single supramaxilla, a 'V'-shaped median rostral with lateral horns and an interopercle that lies in series with the subopercle (rather than underlying the preopercle and subopercle as in teleosts). Some of these characters may turn out to be characters of a more inclusive group such as Halecostomi (Halecomorphi + Teleostei) but their taxonomic distribution needs more precise documentation. For instance a double jaw joint has been described for the aspidorhynchid *Vinctifer comptoni* by Brito (1988), a fish normally regarded as a teleost. The symplectic is very long but apparently fails to articulate with the lower jaw (Brito 1988: 822). Of course, such a structure may mean that aspidorhynchids should be regarded as halecostomes. At the very least a thorough survey of aspidorhynchid jaw articulations is necessary before the homology and heirachical significance of the double jaw joint can be assessed. Grande & Bemis (1998) have carried out the most comprehensive survey of taxa within halecomorphs and provided a character list and data matrix. Their matrix was designed to establish the interrelationships of taxa within the single family Amiidae but they included a sample of taxa from other

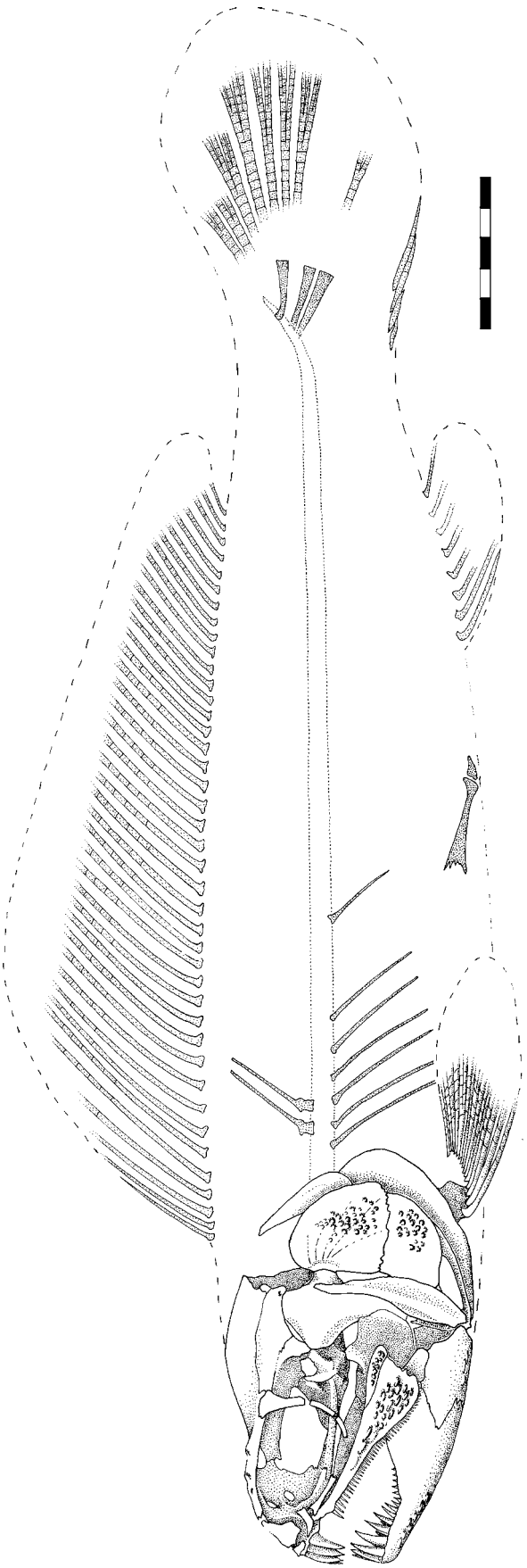

**Figure 19** †*Tomognathus mordax* Dixon, 1850. Reconstruction of the entire fish. Proportions based on BMNH P.10632. Scale bar = 20 mm.

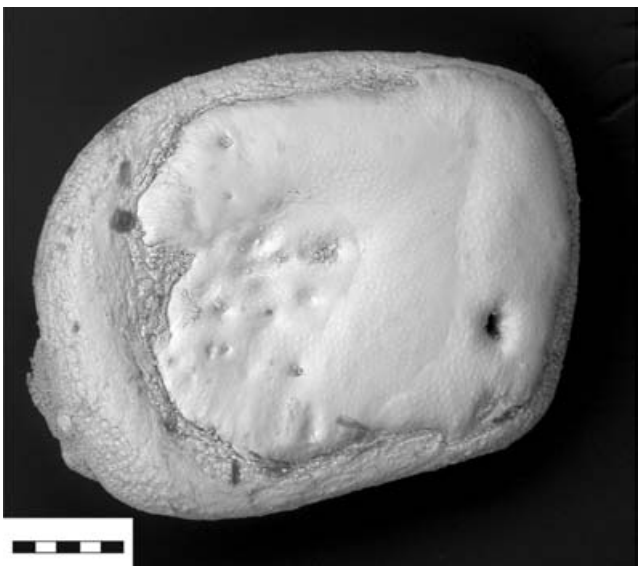

**Figure 20** †*Tomognathus mordax* Dixon, 1850. Scanning electron microscope images of possible scales belongong to †*Tomognathus*. These scales were removed from near the caudal peduncle of BMNH P.10632. Their orientation in life is unknown. Scale bar = 100 $\mu$m.

recognised subgroups of halecomorphs. In trying to establish the relationships of †*Tomognathus* within the halecomorphs we use the matrix generated by Grande & Bemis, listing their characters in their wording and justifying the specific codes used. In two cases (characters 17 and 26) we have added additional character states to their characters or changed the codes in order to express similarities between some structures in †*Tomognathus* and taxa that they used. Such additions are identified in the character descriptions by an asterisk preceeding the character number. In what follows we specify the state shown by †*Tomognathus* in parentheses. Unfortunately much of the postcranial skeleton is currently unknown for †*Tomognathus* and inevitably there are more question marks than we would wish for against this taxon, causing difficulty in the computer cladistic analysis (see below). However, sufficient evidence is present to justify the phylogenetic placement of †*Tomognathus* as Superfamily Amioidea *incertae sedis*.

## Character coding

The character codes used for †*Tomognathus* and added to the matrix of Grande & Bemis (1998) are shown in Fig. 21 and justified below.

1. Solid, perichordally ossified, diplospondylous centra in adult-sized individuals. (0 = absent; 1 = present). †*Tomognathus* has only questionable remains as centra. (?)
2. Posterior extent of exoccipitals in adult-sized individuals. (0 = reaches posterior margin of occiput; 1 = does not reach posterior margin of occiput). This character relates to the possibility that one or more centra have been incorporated in to the occipital condyle. All amiids show state '1', while most non-amiid halecomorphs examined by Grande & Bemis (1998) show state '0', as do primitive teleosts. †*Tomognathus* clearly shows state '0' since the exoccipital makes a contribution to the condyle (see Fig. 8A). (0)
3. Anteriorly projecting processes on neural and/or haemal arches. (0 = absent; 1 = present). Condition unknown in †*Tomognathus*. (?)
4. Lateral fossae of vertebral centra of adult-sized individuals. (0 = present, with two pits on each side of most centra; 1 = present with more than three pits on each side of most centra; 2 = absent, centra smooth sided). Condition unknown in †*Tomognathus*. Ossified centra are only questionably present. (?)
5. Number of supraneurals. (0 = ≥15; 1 = 13–14; 2 = 5–11). Condition unknown in †*Tomognathus*. (?)
6. Articular ossification of the lower jaw. (0 = a simple element, or two elements tightly sutured to one another; 1 = two separate elements not in contact with one another). Grande & Bemis (1998) noted that in *Amia*, †*Calamopleurus cyclindricus* Agassiz, 1841, †*Pachyamia mexicana* Grande & Bemis, 1998 and †*Cyclurus kehreri* (Andreae, 1893) – taxa placed within their supersubfamily Amiista – the articular of the lower jaw is ossified as anterior and posterior elements. The quadrate articulates with the anteriorly placed articular, the symplectic with the posterior articular. †*Tomognathus* shows the plesiomorphic condition of having a single articular ossification (see Fig. 12C). It also shows that the quadrate and symplectic articulations lie very close to one another (see Fig. 12D). This too appears to be the plesiomorphic condition within halecomorphs. Among those fossil taxa listed above that have two articular bones then †*Cyclurus kehreri* appears, uniquely, to be like *Amia* in that the quadrate and symplectic articulations lie well separated from one another (Grande & Bemis 1998: figs 49 and 152). (0)
7. Presence/absence of suborbital bones. (0 = one or more present; 1 = absent). The presence of suborbital bones is plesiomorphic within neopterygians. †*Tomognathus* lacks a suborbital (state 1), as do more derived amiids. We note, however, that the absence of a suborbital from the cheek of †*Tomognathus* is clearly related to the general reduction of bones surrounding the eye where the infraorbitals are reduced to small tube-like elements and there are no supraorbitals. This extreme reduction appears to be unique to †*Tomognathus* among halecomorphs. (1)
8. Strength of ornamentation on dermal bones of skull. (0 = weak and/or fine; 1 = strong, coarse). Grande &

```
                                  11111111112222222222333333333344444444445555555556666666666
                        1234567890123456789012345678901234567890123456789012345678901234567890123456789
†Tomognathus mordax     ?0???010??01?1202N?10??0120??0?00N00N00??02?1??1?0110??010001101?N?11
```

**Figure 21** Data for †*Tomognathus mordax* as added to the matrix of Grande & Bemis (1998).

Bemis acknowledge the subjective nature of variation expressed in this character but they do illustrate their meaning, using operculae of various amiid taxa. †*Tomognathus* shows dermal bones that are nearly smooth (see Fig. 15). Only the maxilla, anteroventral portion of the dentary, angular and parts of the operculum, subopercle and gular (see Fig. 14) are ornamented with discrete tubercles. Therefore, this corresponds to state '0'. (0)

9. Hypural–ural centra fusion in adult-sized individuals. (0 = all hypurals autogenous (separate) from the ural centra; 1 = all but the first hypural fused to corresponding centra). The caudal endoskeleton of †*Tomognathus* is too poorly known for comment or assessment of character states. (?)
10. Presence/absence of large parapophyses fused to most of the abdominal centra. (0 = absent; 1 = present). The vertebral column of †*Tomognathus* remains virtually unknown. (?)
11. Presence/absence of substantial scapulocoracoid ossification in adult-sized individuals. (0 = one or more elements present in the shoulder girdle; 1 = absent). Although the scapulocoracoid is very poorly known (see Fig. 16) sufficient remains to establish that some degree of ossification was present. (0)
12. Presence/absence of supraorbital bones. (0 = two or more present; 1 = absent). Grande & Bemis (1998: 576) noted the two conditions listed here within their halecomorph sample, with the absence of supraorbitals restricted to members of the subfamily Amiinae. †*Tomognathus* has no supraorbitals (see remarks under character 7). (1)
13. Urodermals in the caudal skeleton. (0 = present; 1 = absent). There are no specimens of †*Tomognathus* sufficiently well-preserved to comment. (?)
14. Presence/absence of sclerotic ring ossification. (0 = present; 1 = absent). †*Tomognathus* lacks a sclerotic ring. (1)
15. Size and shape of the dorsal fin. (0 = short, with straight to falcate margin, 14–25 segmented rays and 14–25 proximal radials; 1 = medium long, with bow-shaped or straight margin, 30–34 segmented rays and an estimated 30–34 proximal radials; 2 = very long, with bow-shaped margin, 36–47 segmented rays and 37–48 proximal radials; 3 = extremely long, with bow-shaped margin, 48–53 segmented rays and 49–54 proximal radials). Grande & Bemis (1998: 577) identified four states of variation of dorsal fin shape that, in combination, describe shape and length. One of their states ('0') describes a short fin (14–25 segmented rays) with a straight to falcate margin. The other three states define medium or long, straight or bow-shaped fins: the states being distinguished by the number of rays. The dorsal fin of †*Tomognathus* corresponds most closely with their state '2' (very long, with bow-shaped margin, 36–47 segmented rays) and this is how we choose to code it. In fact, the dorsal fin of †*Tomognathus* may be considered autapomorphic in the sense that it begins immediately behind the head, there being little or no gap between the occiput and its origin. There may therefore be a case for suggesting a fifth state, exclusive to †*Tomognathus*. Grande & Bemis (1998: 577) also make the point that the length of the fin may be decoupled from the number of supporting elements. In *Amia calva* the fin rays lie in series with the pterygiophores that, in turn, lie in one-to-one series with the neural spines. This is not the case in †*Vidalamia catalunica* (Sauvage, 1903) as shown by Grande & Bemis (1998: fig. 250). (2)
16. Morphology of teeth on anterior coronoid and vomer. (0 = conical, with pointed tips; 1 = styliform, with broadly rounded or flattened tips; N = no anterior coronoid). †*Tomognathus* clearly has state '0' (see Fig. 12B). (0)

*17. Anterior extent of parasphenoid tooth patch. (0 = extends well anterior to the lateral ascending arms of the parasphenoid; 1 = short, does not extend anterior to the ascending arms of the parasphenoid; 2 = parasphenoid tooth patch absent). Grande & Bemis (1998: 578) recognise three states. Two described the extent of teeth while the third they scored as 'Not Applicable' to describe the absence of teeth. In their taxon sampling this code is used only for the teleost †*Pholidophorus macrocephalus* Agassiz, 1833–1844. The presence of parasphenoid teeth is a plesiomorphic condition for actinopterygians and we consider the recording of absence to have potential grouping significance. Therefore we use this character and replace the 'N' code with state '2'. (2)

18. Parietal length. (0 = relatively long, with a width-to-length ratio range not exceeding 0.90; relatively short, with a width-to-length ratio well exceeding 0.90). Grande & Bemis (1998: 578) recognise two states of parietal dimension, using a Non-Applicable code for members of the †Sinamiidae that have median parietals. We therefore code Non-Applicable for †*Tomognathus*. (N)
19. Number of ural centra. (0 = 10 or fewer; 1 = 11–22). Unknown for †*Tomognathus*. (?)
20. Shape of preopercle. (0 = L-shaped; 1 = crescent-shaped; 2 = crescent-shaped, wide in middle, tapering dorsally and ventrally; 3 = ovoid). Grande & Bemis (1998: fig. 242) illustrate two of the states of this four-state character. The preopercle of †*Tomognathus* most closely corresponds with that of †*Oshunia brevis* Wenz & Kellner, 1986 in being crescent-shaped with a slightly expanded ventral end (see Fig. 15). We therefore use a coding similar to that for *Oshunia*. (1)
21. Morphology of caps of jaw teeth in adult-sized individuals. (0 = round in cross-section, not sharply carinate; 1 = labiolingually compressed, sharply carinate (keeled)). †*Tomognathus* shows rounded, non-carinate teeth (e.g. Fig. 5B). (0)
22. Lateral edge of posttemporal in adult-sized individuals. (0 = shorter than length of anterior edge; 1 = elongate, about equal to or greater than width of anterior edge). The posttemporal is unknown in †*Tomognathus*. (?)
23. Shape of posterior margin of caudal fin. (0 = forked; 1 = convexly rounded; 2 = straight and nearly vertical). The only specimens showing any of the caudal fin rays is BMNH P.10632 (see Fig. 17; Woodward 1908: pl. 29, fig. 13). Of this specimen Woodward writes (1908: 142) '. . . . The caudal fin (*c*.) consists of very stout, closely articulated, and finely divided rays; and their remains shown in fig. 13 suggest that was not forked.' This is probably true but it is impossible to identify whether

it is convexly rounded or straight. In view of the very incomplete preservation we leave it as questionable. (?)

24. Elongation of the opercular process of the hyomandibular. (0 = absent; 1 = present). †*Tomognathus* shows a barely differentiated opercular process (see Figs 10C & 12D). (0)
25. Number of tooth rows on coronoids. (0 = two or more rows for at least part of one or more coronoids; 1 = one row; N = no coronoids). †*Tomognathus* shows only a single coronoid (we deal with this below), where the teeth are aligned in a single row and hence shows state 1 with respect to tooth alignment. (1)
*26. Arrangement of vomerine teeth. (0 = tooth patch with two to several rows of teeth; 1 = tooth patch with only a single marginal row, plus one or more teeth in a longitudinal series perpendicular to the anterior marginal row; 2 = tooth patch arranged as a single transverse row). Grande & Bemis (1998) established the first two states of this character to differentiate a very specific pattern in †*Calamopleurus* and †*Maliamia* (Grande & Bemis 1998: figs 309, 321) as state '1'. †*Tomognathus* shows just a few teeth aligned in a single row approximately transversely (see Fig. 5B). We therefore added a third state (coded as '2') to this character since it has elements of the other two states. We also note here that †*Tomognathus* appears to be uniquely derived amongst halecomorphs to show a median, unpaired vomer, a condition more usually seen in teleosts. (2)
27. Presence/absence of dermopterotic ribs. (0 = absent; 1 = present). Such ribs are absent from †*Tomognathus*, as they are from most halecomorphs. (0)
28. Number of epurals. (0 = 2–8; 1 = 10–15). This region of the body is unknown in †*Tomognathus*. (?)
29. Shape of basipterygium. (0 = proximal end flat and widened anteriorly; 1 = proximal end long and rod-like, without significant widening anteriorly). This region of the body is poorly known in †*Tomognathus*. (?)
30. Postmaxillary process under postmaxillary notch. (0 = tiny or absent; 1 = thick and elongate). Grande & Bemis (1998: fig 243) give outline drawings of the maxillae in a variety of halecomorphs and designate two states, one of which they assign to †*Vidalamia* and †*Pachyamia* in which the notch in the posterior margin of the maxilla (characteristic of all halecomorphs) is particularly well developed and in which the lower limb demarcating the notch is thickened. There is considerable variation in the shapes designated as state '0' and that in †*Tomognathus* falls well within this variation, being most similar to that of †*Solnhofenamia* and †*Amiopsis*. (0)
31. Morphology of pleural ribs. (0 = distal ends pointed or without rounded points; 1 = distal ends flatly truncated, even in large adults). Ribs are poorly known in †*Tomognathus*. (?)
32. Shape of gular. (0 = subtriangular or subrectangular with acute rounded anterior apex; 1 = broad, oval, without acute anterior apex). Grande & Bemis (1998: fig. 136) separate the rounded gular plate of †*Vidalamia* and †*Pachyamia* as state '1', all others being a variation on their description of state '0'. We note that the shape of the gular in †*Tomognathus* is remarkably similar to that of †*Calamopleurus* (see Fig. 14 and see below, character 64). (0)
33. Peculiar ornamentation of strongly defined, converging lines on opercles in adult-sized individuals. (0 = absent; 1 = present). The ornament upon the opercle of †*Tomognathus* is best described under state '0'. We note that the shape of the opercle appears to be unique among halecomorphs in showing an irregular and partly serrated ventral margin (see Fig. 15). (0)
34. Frontal width in adult-sized individuals. (0 = relatively wide, with a width-to-length ratio of 0.26–0.65; 1 = relatively narrow, with a width-to-length ratio of 0.13–0.21). The frontals are fused in †*Tomognathus*, hence this character is scored as 'Not Applicable'. (N)
35. Shape of dermopterotic. (0 = greatly widened posteriorly and tapered anteriorly; 1 = subrectangular, not substantially tapered anteriorly or expanded posteriorly). The dermopterotic of †*Tomognathus* narrows anteriorly (see Fig. 3), corresponding to state '0'. (0)
36. Width of opercle. (0 = narrow, with width-to-height ratio 0.56–1.06; 1 = wide, with width-to-height ratio in the range of 1.07–1.39). The opercle of †*Tomognathus* is approximately equidimensional (see Fig. 15), most like that of †*Cyclurus* and *Amia* (Grande & Bemis 1998: fig. 180A-K). (0)
37. Presence of an interfrontal fontanelle in adult-sized individuals. (0 = absent, frontals sutured to each other medially for their entire length; 1 = frontals separated for about one half of their length or more by a fontanelle). The frontals of †*Tomognathus* are fused and therefore this character must be scored as Not Applicable'. (N)
38. Position of dermosphenotic relative to orbit in adult-sized individuals. (0 = anterior or anteroventral margin of dermosphenotic included in circumorbital margin, even in large adults of 200 mm standard length (SL) or more; 1 = dermosphenotic excluded from orbital margin in large individuals of 200 SL or more). The dermosphenotic of †*Tomognathus* is included in the orbital margin and lies anterior to the dermopterotic. (see Fig. 15 and Woodward 1908: fig. 7). (0)
39. Shape of supramaxilla. (0 = elongate; 1 = extremely deep, shaped like a rounded triangle). †*Tomognathus* has an elongate supramaxilla (see Figs 11C & 15; cf. Grande & Bemis 1998: fig. 277 for state 0). (0)
40. Number of preural vertebrae (preural centra = abdominal plus preural caudal centra). (0 = 40–73; 1 = 75–82). Centra poorly known in †*Tomognathus*. (?)
41. Shape of posterior end of posttemporal in adult-sized individuals. (0 = elongate, with rounded apex or apices; 1 = elongate but abruptly truncated). Posttemporal unknown in †*Tomognathus*. (?)
42. Ventral transverse ridge of gular. (0 = absent; 1 = present). This character was identified as autapomorphic for †*Pachyamia mexicana* by Grande & Bemis (1998). †*Tomognathus* lacks such a ridge. (0)
43. Shape of anterior subinfraorbital bone in adult-sized individuals. (0 = short, subrectangular, longer than deep; 1 = subrectangular, deeper than long; 2 = long, very thin, tube-like; 3 = posteriorly expansive, tapering anteriorly). †*Tomognathus* shows a small tube-like anterior subinfraorbital (called infraorbital 1 here – see Fig. 15). (2)

44. Number of epaxial procurrent caudal fin rays. (0 = 0–11; 1 = 12–15). The caudal fin of †*Tomognathus* is insufficiently known to code. (?)
45. Presence/absence of fringing fulcra on median fins. (0 = present; 1 = absent). Although the dorsal fin is only partly known there appear to be no fringing fulcra in †*Tomognathus*. The other median fins are unknown. (1)
46. One-to-one arrangement of hypurals and caudal fin rays. (0 = last few hypurals each articulate with the bases of several fin rays; 1 = each hypural normally bears a single caudal ray). The caudal fin of †*Tomognathus* is insufficiently known to code. (?)
47. Number of ossified ural neural arches. (0 = normally four or more; 1 = normally two or fewer). The caudal fin of †*Tomognathus* is insufficiently known to code. (?)
48. Number of parietal bones. (0 = paired parietals normally present; 1 = only a single median parietal present). †*Tomognathus* has a median parietal (see Fig. 3). (1)
49. Number of pairs of extrascapular bones. (0 = only one pair present; 1 = three pairs normally present). Extrascapulars are unknown in †*Tomognathus*. (?)
50. Dermopterotic length to parietal length. (0 = dermopterotic significantly longer; lengths about equivalent = 1). Grande & Bemis (1998) illustrate what they mean by these dimensions and †*Tomognathus* corresponds with state '0' (see Fig. 3). (0)
51. Presence/absence of opisthotic. (0 = present; 1 = absent). †*Tomognathus* lacks an opisthotic (see Fig. 6). (1)
52. Presence/absence of pterotic. (0 = present; 1 = absent). †*Tomognathus* lacks an (auto)pterotic (see Fig. 6). (1)
53. Shape of maxilla extremely slender and rod-like. (0 = no; 1 = yes). Based on illustrations specifying these states (Grande & Bemis 1998: fig. 243) †*Tomognathus* shows state '0'. (0)
54. Number of branchiostegal rays. (0 = 21 or fewer; 1 = 22 or more). The branchiostegal ray series of †*Tomognathus* is very poorly known. It is known to show a branchopercle, preceded by at least three filamentous branchiostegals but the exact number is not known. (?)
55. Numerous paired block-like ural neural arch ossifications. (0 = absent; 1 = present). The caudal fin of †*Tomognathus* is insufficiently known to code. (?)
56. Dermosphenotic attachment to skull roof in adult-sized individuals. (0 = loosely attached on the skull roof or hinged to the side of skull roof; 1 = firmly sutured into the skull roof and forming part of it). †*Tomognathus* shows a free dermosphenotic (see Fig. 15). (0)
57. Shape of rostral bone. (0 = plate-like or short tube-like, without lateral horns; 1 = roughly V-shaped, with lateral horns). †*Tomognathus* shows state '1' (see Fig. 13). (1)
58. Lachrymal shape. (0 = longer than deep and smaller than orbit; deeper than long and massive about size of orbit = 1)). The lachrymal (infraorbital 1) of †*Tomognathus* is small and therefore corresponds most closely to state '0' (see Fig. 15). (0)
59. Posterior extent of maxilla. (0 = extends to below the posterior orbital margin; 1 = does not extend below posterior orbital margin). In †*Tomognathus* the maxilla extends to a level posterior to the rear of the orbit (see Fig. 15). (0)
60. Presence/absence of lateral line canal in maxilla. (0 = absent; 1 = present). †*Tomognathus* lacks a lateral line in the maxilla. (0)
61. Symplectic involvement in jaw joint. (0 = does not articulate with lower jaw; 1 = distal end articulates with articular bone of the lower jaw). The symplectic, quadrate and the nature of the jaw joint of †*Tomognathus* is described (p. 11) and illustrated (see Fig. 12D) to show the involvement of the symplectic in the lower jaw joint. (1)
62. Shape of posterior margin of the maxilla. (0 = convexly rounded or straight; 1 = excavated (concave or with a posterior maxillary notch present)). Shapes of the posterior end of the maxilla in a range of halecomorph taxa, all of which show state '1', are illustrated by Grande & Bemis (1998: fig. 243). That of †*Tomognathus* (see Fig. 11B) most closely corresponds to that of †*Amiopsis* spp, the chief difference being that the margin is serrated in †*Tomognathus*. (1)
63. Innerorbital flange of dermosphenotic. (0 = smooth, without sensory canal; 1 = bearing sensory canal tube). The sensory canal runs within the main body of the dermosphenotic in †*Tomognathus* and this taxon therefore lacks an innerorbital flange, corresponding to state '0'. (0)
64. Posterior margin of gular. (0 = smooth; 1 = deeply scalloped). In Grande & Bemis' (1998) analysis a gular with a scalloped margin was identified as a synapomorphy of species of †*Calamopleurus*. †*Tomognathus* is now known to possess an almost identically shaped gular (see Fig. 14). (1)
65. Shape of the haemal spines. (0 = spine-like or rod-like; 1 = broadly spatulate in the transverse plane). †*Tomognathus* is insufficiently known for reliable coding. (?)
66. Relative size of uppermost postinfraorbital in adult-sized individuals. (0 = short, much shorter than lowermost postinfraorbital; 1 = long, about equal in length to lowermost postinfraorbital). This character is problematic for †*Tomognathus*. Grande & Bemis (1998) noted a clear difference between those taxa in which the broad plate-like postinfraorbitals were of equal size (e.g. *Amia*) and those in which they were not (e.g. †*Calamopleurus*). †*Tomognathus* differs from all halecomorphs considered by them in that all infraorbitals (postinfraorbitals included) are reduced to small tube-like structures. Therefore, considering this character at face value we would say that †*Tomognathus* shows state '1'. However, in view of the autapomorphic condition of the infraorbitals in this taxon we prefer to code 'Not applicable'. (N)
67. Orientation of preural haemal and neural spines near caudal peduncle. (0 = positioned at about 25–45° from the horizontal; 1 = strongly inclined to nearly horizontal). These structures are unknown for †*Tomognathus*. (?)
68. Presence/absence of interopercle. (0 = absent; 1 = present). †*Tomognathus* has an interopercle (see

Fig. 15). We would also remark that as in all halecomorphs this bone lies in series with the subopercle and does not underlay the preopercle and subopercle as in teleosts. (1)

69. Number of supramaxillae. (0 = none; 1 = one; 2 = two). †*Tomognathus* has a single supramaxilla (see Figs 11C, 15). (1)

## Phylogenetic analysis

†*Tomognathus* has 28 question marks against characters considered here. These question marks denote missing data and non-applicable data. This is a high percentage of question marks (40%) and causes trouble for computer generated phylogenies because it leads to decay of the resolution given by known data, although it needs to be stressed that the question marks do not lead to new topologies. In order to lessen the effect of this high percentage of missing data it was decided that the taxon sampling be reduced to the minimum following the advice of Grande & Bemis (1998: 567–568). This means that all taxa that showed redundancy (that is, their real codes did not add variation to the complement of real data against all taxa), were stripped out. As a result, only the 24 taxa used by Grande & Bemis were used, with †*Tomognathus* being added as a *25th*. Nevertheless, it should be pointed out that even with this reduced taxon sampling we still ran into the perils of optimisation and spurious nodes (detailed below).

The data matrix was analysed using PAUP* 4.0b10 (Swofford 2001) with the characters unordered; †*Eurycormus*, *Atractosteus*, †*Pholidophorus bechei* and †*P. macrocephalus* were used as the outgroup and the branch and bound tree-searching algorithm was employed.

The first analysis omitted †*Tomognathus* in order to check the results against those of Grande & Bemis (1998) since the coding of one character (see character number 17 above) had been changed. Four trees were obtained at 115 steps (one more than Grande & Bemis), the strict consensus of which is shown in Fig. 22 and the tree statistics are given in the legend. The results obtained were in topological agreement with those of Grande & Bemis, with the exception that †*Solnhofenamia elongata* collapsed to a trichotomy with †*Amiopsis lepidota* and the remainder of the Amiidae (in Grande & Bemis' analysis this taxon was resolved as the sister taxon to all remaining Amiidae except †*Amiopsis lepidota*).

The addition of †*Tomognathus* caused a major collapse of taxa within the Superfamily Amioidea to result in the strict consensus of 24 trees showing an eight-fold multifurcation (Fig. 23). Even more surprising was the fact that the sistergroup pairing of †*Cyclurus gurleyi* with the three included species of †*Amia* was now included in a polytomy (previously it had been calculated that the node †*Cyclurus gurleyi* + *Amia* spp. had a Bremer support of 8). However, inspection of alternative placements for †*Tomognathus* in the fundamental trees demonstrate that the collapse is largely illusory and must be viewed as having little significance. Within the 24 fundamental trees, †*Tomognathus* is placed at five positions as shown in Fig. 24. Two of these positions are sistergroup pairings with terminal taxa, a third is as sistergroup to *Amia* spp. and a fourth is as sistergroup to the sinamiid taxa; hence, the collapse of the amioid clade in the strict consensus tree when †*Tomognathus* is included. Closer inspection of each of these alternatives shows very little support by real data.

The node (†*Tomognathus* + †*Cyclurus gurleyi*) is supported by character changes in three characters, namely 6 (1 → 0, CI (consistency index) = 0.500) 17 (0 → 1, CI = 0.667), 18 (0 → 1, CI = 0.200). †*Tomognathus* is coded as question marks for 6 and 18. Secondly, these two taxa differ in the codings for character 17 and the node state is only resolved by ambiguous optimisation. This must be regarded as a spurious node.

The node (†*Tomognathus* (*Amia* spp.)) is only supported by one character change – 40 (0 → 1, CI = 0.500); this character is coded as a question mark for †*Tomognathus* and therefore this node is spurious.

The node (†*Tomognathus*, †*Amia pattersoni*) is supported by two character changes – 6 (1 → 0, CI = 0.500) and 25 (0 → 1, CI = 0.500), both of which characters are coded as question marks for †*Amia pattersoni*, so once again this must be regarded as a spurious node.

The node (†*Tomognathus* (†*Cyclurus gurleyi* + *Amia* spp.)) is supported by eight character changes – 5 (1 →2, CI = 0.667), 9 (0 → 1, CI = 1.000), 10 (0 → 1, CI = 0.500), 12 (0 → 1, CI = 1.000), 13 (0 → 1, CI = 1.000), 14 (0 → 1, CI = 0.500), 15 (0 → 2, CI = 0.750), 66 (0 → 1, CI = 1.000). Of these character changes, numbers 9, 12, 13 and 66 are optimised as synapomorphies. However, †*Tomognathus* is coded as question marks for 9, 13 and 66 (as well as 5 and 10). Therefore, the only unambiguous character suggesting that †*Tomognathus* is more closely related to †*Cyclurus gurleyi* and *Amia* spp. is the '1' state of character 12 – the shared absence of supraorbital bones. While this is true it should be noted that the pattern of the remaining cheek bones in †*Tomognathus* is highly apomorphic among the halecomorphs considered here in being reduced to tiny tube-like elements. Parenthetically it should be noted that this is the result obtained when the characters were reweighted (using the rescaled consistency index with a baseweight of 1000 applied).

The node (†*Tomognathus* (†*Sinamia zdanskyi*, †*Ikechaoamia meridionalis*) is supported by seven character changes – 7 (0 → 1, CI = 0.500), 14 (0 → 1, CI = 0.333), 17 (0 → 2, CI = 0.667), 22 (0 → 1, CI = 0.500), 26 (0 → 2, CI = 0.400), 48 (0 → 1, CI = 1.000), 49 (0 → 1, CI = 0.500). †*Tomognathus* shows question marks for two of these characters (22 and 49), while †*Sinamia zdanskyi* and †*Ikechaoamia meridionalis* are coded as question marks for characters 7, 14, 17 and 26. There is one synapomorphy that suggests this sistergroup pairing: character 48 – fusion of parietals to a median element.

Character changes supporting the Superfamily Amioidea are 23 (0 → 1, CI = 0.500), 45 (0 → 1, CI = 1.000) and 46 (0 → 1, CI = 0.500). Characters 23 and 46 are coded as question marks in †*Tomognathus*, leaving 45 (state 1) – the absence of fringing fulcra on median fins – as the only evidence for the most inclusive position of †*Tomognathus*.

With the evidence before us there are two phylogenetic positions that are recovered through the computer parsimony analysis that can be justified by real data; either †*Tomognathus* is the sistergroup to sinamiids, or the sister group to *Cyclurus gurleyi* + *Amia* spp.

Somewhat disturbingly, it should be noted that global parsimony failed to identify two synapomorphies that place †*Tomognathus* as the sister group to †*Calamopleurus*.

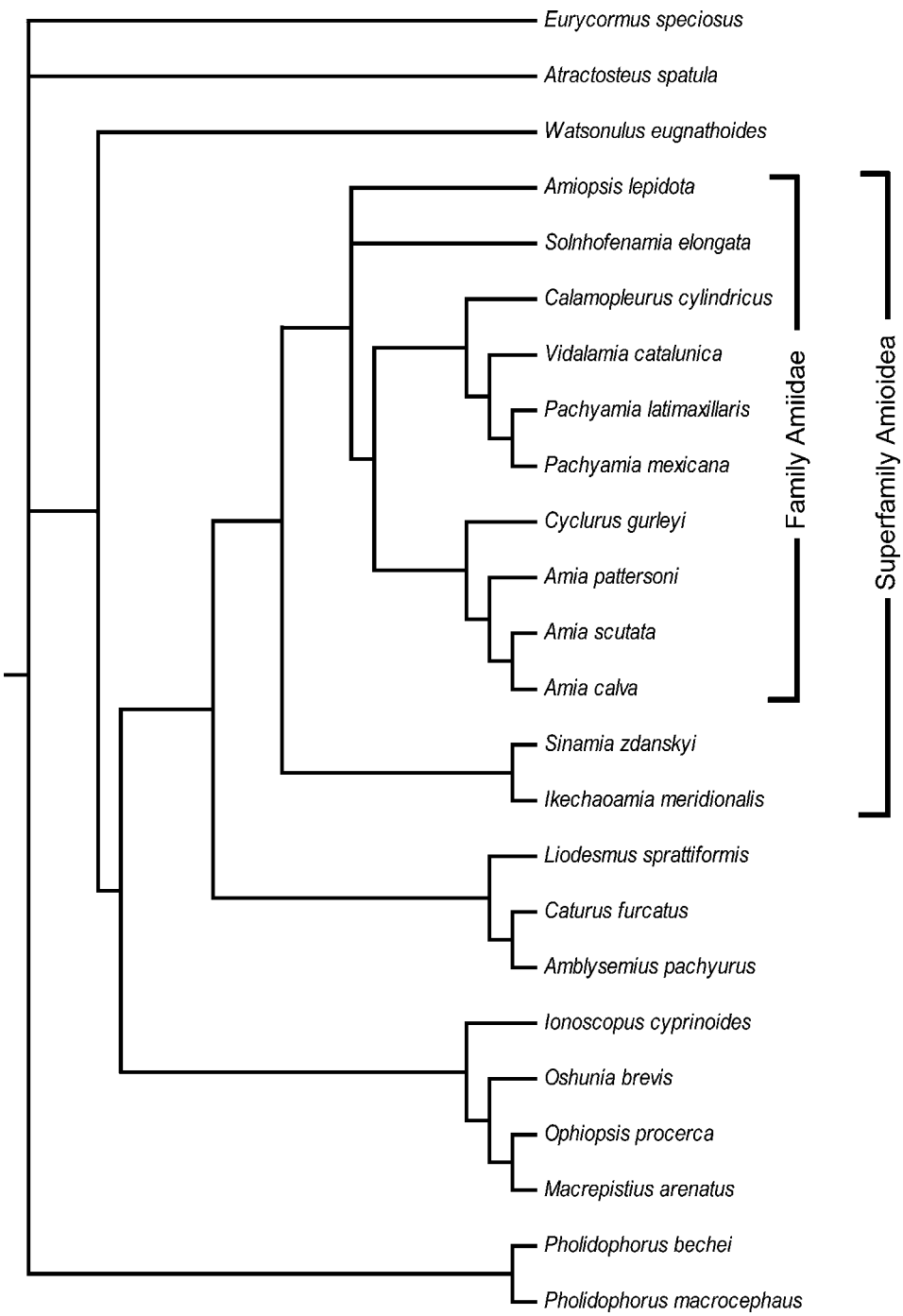


**Figure 22** Result of analysing the reduced data set of Grande & Bemis (1998) using PAUP* version 4.0b10 (Swofford 2001). The coding for one character was changed (see discussion of character 17); all characters are unordered and of equal weight. Strict consensus tree of four trees: length = 115, consistency index (CI) excluding uninformative characters = 0.6667, retention index (RI) = 0.5884.

†*Tomognathus* and the two species of †*Calamopleurus* are unique among the taxa considered here in having a single row of teeth upon the coronoid (character 25, state 1) and in having the posterior edge of the gular plate deeply scalloped (character 64, state 1). A third character – dermosphenotic loosely attached to the skull roof (character 56, state 0) – is also shared with †*Calamopleurus*, but this is also found in non-halecomorphs and †*Watsonulus* among the taxa considered here. All of these observations are recorded in the data matrix but any grouping criteria on these character-states disappears amongst global parsimony.

This case study is offered as a salutary reminder that maximum parsimony analysis is fraught with interpretive problems. Care must be taken when interpreting a phylogenetic hypothesis. Of course it would have been possible 'load to the dice' by differential weighting of characters. Without more information about †*Tomognathus*, especially the postcranial skeleton, then we are reluctant to overstretch

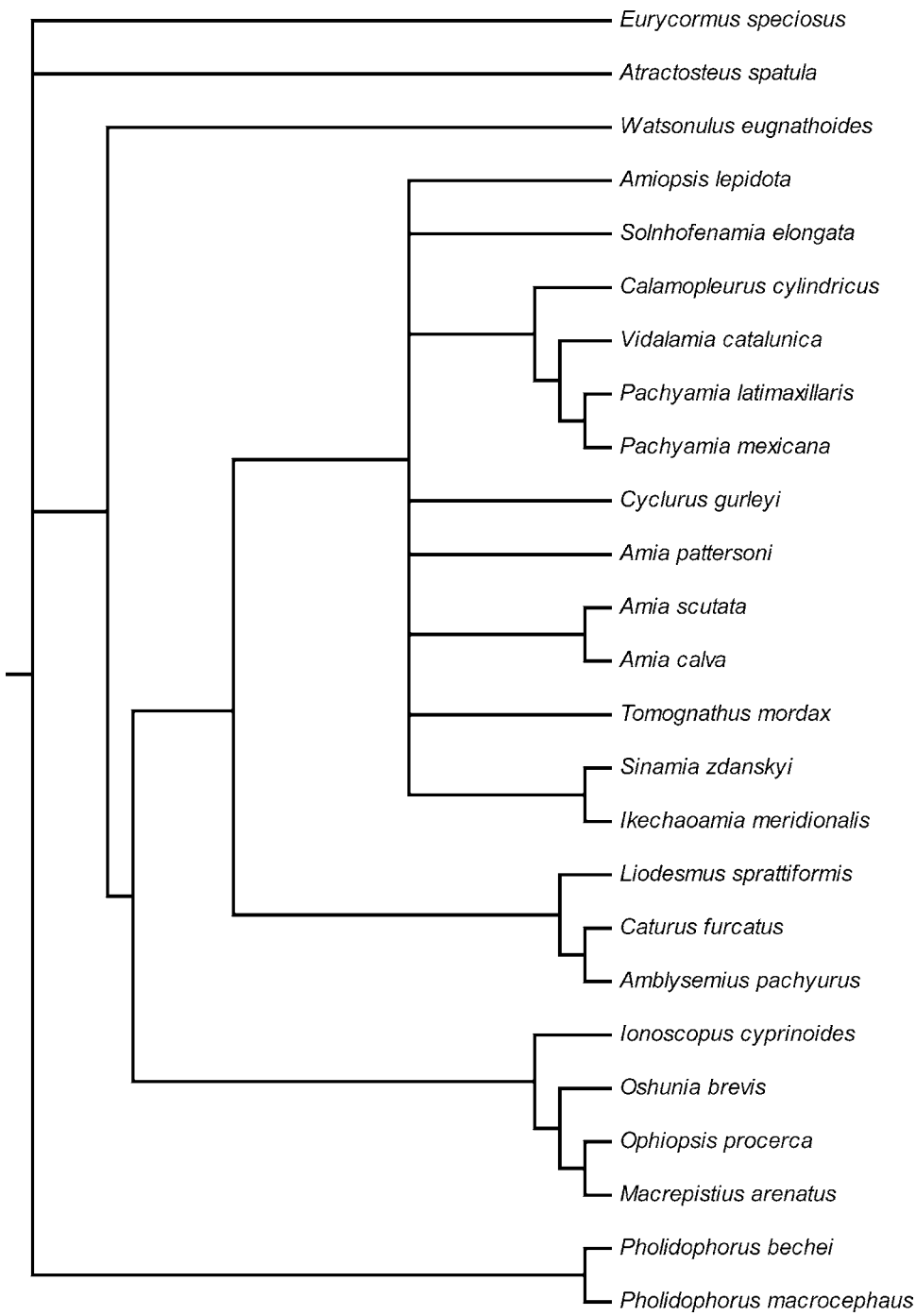


**Figure 23** Result of analysing the reduced data set of Grande & Bemis (1998) using PAUP* version 4.0b10 (Swofford 2001) and including †*Tomognathus*. Strict consensus of 24 trees: length = 125, CI excluding uninformative characters = 0.6303, RI = 0.5282.

the evidence and place this taxon as Superfamily Amioidea *incertae sedis*.

## Conclusions

†*Tomognathus* is one of only three halecomorph fishes that are found in the Upper Cretaceous of England; the other two being †*Lophiostomus dixoni* Egerton, 1852, †*Neorhombolepis excelsus* Woodward, 1888, and †*N*. (?) *punctatus* Woodward, 1895 (Woodward 1909: 160 cast doubt on the generic identity as this species is only based on a few isolated scales). Both †*Lophiostomus dixoni* and †*Neorhombolepis excelsus* are known from very few specimens (in both cases the holotype plus a few isolated pieces) and their relationships are in doubt. Both were originally referred to the †Eugnathidae (=†Caturidae = †Furidae) by Woodward 1909. It has been suggested that †*Neorhombolepis* is a member of the †Ophiopsidae (Grande & Bemis 1998: 607) and that †*Lophiostomus dixoni* should also be removed

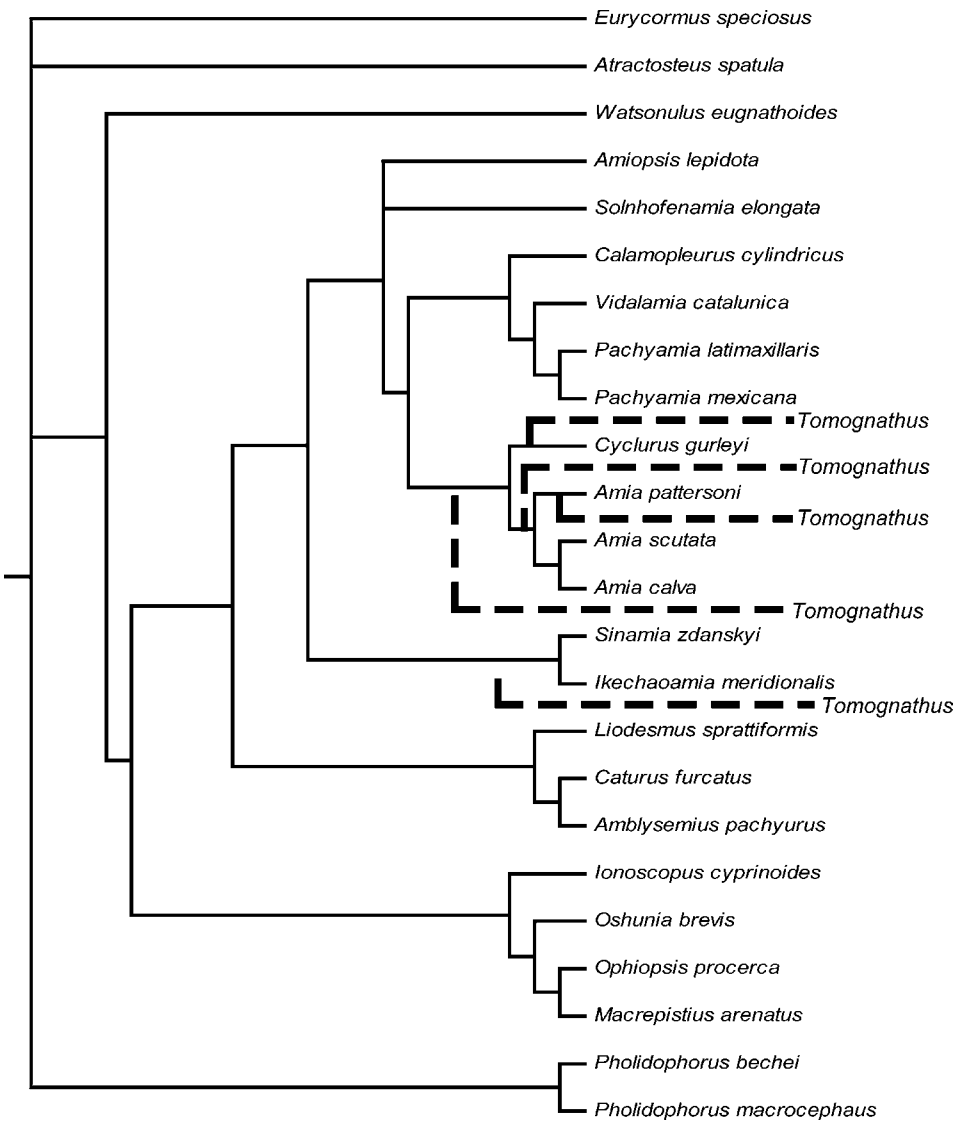


**Figure 24** Alternative resolutions for †*Tomognathus* among the 24 trees obtained in Fig. 23. See the text for discussion of character support for each position.

from the family (Bartram 1975). Despite the fact that both of these taxa are left in limbo pending a comprehensive revision of caturid fishes no-one has suggested that they are related to fishes outside the Halecomorphi. Halecomorphs are a clade of predaceous fishes that originated in the Lower Triassic and were very common in the Jurassic and Lower Cretaceous. By the Upper Cretaceous, most were confined to freshwater where they flourished until the Oligocene, from when they declined to leave *Amia calva* (the bowfin of the eastern USA) as the sole representative. Among halecomorphs, †*Tomognathus* is certainly one of the most unusual and among the last of the marine representatives. The high degree of fusion of skull roof bones, the extreme reduction of the cheek bones and the naked body is unique within this clade, as is the weakness, or absence of ossification of the centra. The characters that are available place it as a member of the Superfamily Amioidea and with these fishes it shares the overall form of the body.

## Acknowledgements

We would like to thank John Cooper, Booth Museum, Brighton; Jenny Clack, Museum of Zoology, Cambridge University and Rod Long, Sedgwick Museum, Cambridge University for the loan of material. We also extend our thanks to Phil Crabb and Alison Longbottom, The Natural History Museum, for their skills in taking the photographs and composing the electronic figures, respectively. We also thank our two reviewers, Dr John Maisey (American Museum of Natural History) and Dr Paulo Brito (Universidade do Estado do Rio de Janeiro, Brazil) for corrections and suggestions.

## References

**Agassiz, J. L. R.** 1833–1844. *Recherches sur les Poissons Fossiles,* vol. 1. Petitpierre, Neuchatel, 188 pp.

**Andreae, A.** 1893. Vorläufige Mittheilung über die Ganoiden (*Lepidosteus* und *Amia*) des Mainzer Beckens. *Verhandlungen des Natuhistorisch-medizinischen Vereins Heidelberg* **2 (ser 5)**: 7–15.

**Arratia, G.** 1999. The monophyly of Teleostei and stem-group teleosts. Consensus and disagreements. Pp. 265–334 *in* G. Arratia and H.-P. Schultze (eds) *Mesozoic fishes 2 – systematics and the fossil record*. Dr Friedrich Pfei l, München.

**— & Schultze, H.-P.** 1987. A new halecostome fish (Actinopterygii, Osteichthyes) from the late Jurassic of Chile and its relationships. *Dakoterra* **3**: 1–13.

**Bartram, A. W. H.** 1975. The holostean fish genus *Ophiopsis* Agassiz. *Zoological Journal of the Linnean Society of London* **56**: 183–205.

**Bonaparte, C. L.** 1838. Selachorum tabula analytica. *Nuovi Annali della Scienze Naturali, Bologna* **2**: 195–214.

**Bridge, T. W.** 1877. The cranial osteology of *Amia calva*. *Journal of Anatomy* **11**: 605.

**Brito, P. M.** 1988. La structure du suspensorium de *Vinctifer*, poisson actinopterygien Mésozoique: remarques sur les implications phylogénétiques. *Geobios* **21**: 819–823.

**Cope, E. D.** 1872. Observations of the systematic relations of the fishes. *Proceedings of the American Association for the Advancement of Science* **20**: 317–343.

**—** 1887. Geology and paleontology. *American Naturalist* **21**: 1014–1019.

**Dixon, F.** 1850. *The geology and fossils of the Tertiary and Cretaceous members of Sussex*. Richard & John Edward Taylor, London, 442 pp.

**Egerton, P. G.** 1852. Figures and descriptions illustrative of British organic remains. *Lophiostomus dixoni*. *Memoirs of the Geological Survey of the United Kingdom* **Decade 6**: Article 10, 1–7, pls X, X*.

**Ekrt, B.** 2001. *Revize Osteichthyes České křídové pánve*. MSc thesis; Charles University, Prague, 167 pp.

**Fink, W. L. & Weitzman, S. H.** 1982. Relationships of the stomiiform fishes (Teleostei), with a description of *Diplophos*. *Bulletin of the Museum of Comparative Zoology* **150**: 31–93.

**Forey, P. L. & Grande, L.** 1998. An African twin to the Brazilian *Calamopleurus* (Actinopterygii: Amiidae). *Zoological Journal of the Linnean Society of London* **123**: 179–195.

**Fric, A.** 1879. Ueber einem neuen Fisch aus dem Pläner des weissen Berges bei Prag. *Sitzungsberichte der Koniglichen Böhmischen Gesellschaft der Wissenschaften* **1879**: 3–4.

**— & Bayer, F.** 1902. Nové Ryby Ceského útvaru Krídového. *Palaeontographica Bohemiae* **7**: 1–18, 13 pls.

**Fritsch, A. & Bayer, F.** 1905. *Neue Fische und Reptilien aus der Böhmischen Kreideformation*. Selbstverlag, Prague, 34 pp.

**Grande, L. & Bemis, W. E.** 1998. A comprehensive phylogenetic study of amiid fishes (Amiidae) based on comparative skeletal anatomy. An empirical search for interconnected patterns of natural history. *Journal of Vertebrate Paleontology* **Memoir 4**: 1–690.

**Harold, A. S. & Weitzman, S. H.** 1996. Interrelationships of stomiiform fishes. Pp. 333–353 *in* M. L. J. Stiassny, L. R. Parenti & G. D. Johnson (eds) *Interrelationships of fishes*. Academic Press, San Diego.

**Hay, O. P.** 1929. Second bibliography and catalogue of the fossil vertebrata of North America. *Publications of the Carnegie Institute of Washington* **390**: 1–2003.

**Maisey, J. G.** 1999. The supraotic bone in neopterygian fishes (Osteichthyes, Actinopterygii). *American Museum Novitates* **3267**: 1–52.

**Nelson, G. J.** 1973. Relationships of clupeomorphs, with remarks on the structure of the lower jaw in fishes. Pp. 333–349 *in* P. H. Greenwood, R. S. Miles & C. Patterson (eds) *Interrelationships of Fishes*. Academic Press, London.

**Patterson, C.** 1973. Interrelationships of holosteans. Pp. 233–305 *in* P. H. Greenwood, R. S. Miles & C. Patterson (eds) *Interrelationships of Fishes*. Academic Press, London.

**—** 1993. Osteichthyes: Teleostei. Pp. 621–656 *in* M. J. Benton (ed.) *The Fossil Record 2*. Chapman and Hall, London.

**Regan, C. T.** 1912. The osteology and classification of the teleostean fishes of the order Apodes. *Annals and Magazine of Natural History* **10**: 377–387.

**—** 1923. The skeleton of *Lepidosteus*, with remarks on the origin and evolution of the lower neopterygian fishes. *Proceedings of the Zoological Society of London* **1923**: 445–461.

**Rosen, D. E., Forey, P. L., Gardiner, B. G. & Patterson, C.** 1981. Lungfishes, tetrapods, paleontology, and plesiomorphy. *Bulletin of the American Museum of Natural History* **167**: 159–276.

**Sauvage, H. E.** 1903. Noticia sobre los peces de la caliza litográfica de la provincia de Lérida. *Memorias de la Real Academia de Ciencias y Artes de Barcelona, 3rd series* **4**: 467–481.

**Swofford, D. L.** 2001. *PAUP*: phylogenetic analysis using parsimony and other methods*. (Software). Sinauer Associates, Sunderland, Massachusetts.

**Toombs, H. A. & Rixon, A. E.** 1959. The use of acids in the preparation of vertebrate fossils. *Curator* **2**: 304–312.

**Wenz, S. & Kellner, A. W. A.** 1986. Découverte du premier Ionoscopidae (Pisces, Halecomorphi) sud-américain, *Oshunia brevis* n.g, n.sp., dans le Crétacé de la Chapada do Araripe (nord-est du Brésil). *Bulletin Muséum national d'Histoire naturelle, Paris* **8(4) sect. C**: 77–88.

**Woodward, A. S.** 1888. A synopsis of the vertebrate fossils from the English Chalk. *Proceedings of the Geologists Association* **10**: 273–338.

**—** 1895. *Catalogue of the Fossil Fishes in the British Museum (Natural History). Part 3*. British Museum (Natural History), London, 544 pp.

**—** 1901. *Catalogue of the Fossil Fishes in the British Museum (Natural History). Part 4*. British Museum (Natural History), London, 636 pp.

**—** 1908. *The fossil fishes of the English Chalk, Part 4*. The Palaeontographical Society, London, 23 pp.

**—** 1909. *The fossil fishes of the English Chalk. Part 5*. The Palaeontographical Society, London, 31 pp.

**—** 1936. On *Tomognathus*, a teleostean fish from the English Chalk. *Annals and Magazine of Natural History* **17**: 304–306.